Minority Carrier Injection in Epitaxial Schottky Barrier Diodes

by

Shaikh Hasibul Majid

A Thesis Presented to the

FACULTY OF THE COLLEGE OF GRADUATE STUDIES

KING FAHD UNIVERSITY OF PETROLEUM & MINERALS

DHAHRAN, SAUDI ARABIA

In Partial Fulfillment of the
Requirements for the Degree of

MASTER OF SCIENCE

In

ELECTRICAL ENGINEERING

May, 2000

INFORMATION TO USERS

This manuscript has been reproduced from the microfilm master. UMI films the text directly from the original or copy submitted. Thus, some thesis and dissertation copies are in typewriter face, while others may be from any type of computer printer.

The quality of this reproduction is dependent upon the quality of the copy submitted. Broken or indistinct print, colored or poor quality illustrations and photographs, print bleedthrough, substandard margins, and improper alignment can adversely affect reproduction.

In the unlikely event that the author did not send UMI a complete manuscript and there are missing pages, these will be noted. Also, if unauthorized copyright material had to be removed, a note will indicate the deletion.

Oversize materials (e.g., maps, drawings, charts) are reproduced by sectioning the original, beginning at the upper left-hand corner and continuing from left to right in equal sections with small overlaps.

Photographs included in the original manuscript have been reproduced xerographically in this copy. Higher quality 6" x 9" black and white photographic prints are available for any photographs or illustrations appearing in this copy for an additional charge. Contact UMI directly to order.

ProQuest Information and Learning
300 North Zeeb Road, Ann Arbor, MI 48106-1346 USA
800-521-0600

Minority Carrier Injection In Epitaxial Schottky Barrier Diodes

by

Shaikh Hasibul Majid

A Thesis Presented to the
DEANSHIP OF GRADUATE STUDIES

In Partial Fulfillment of the Requirements
for the Degree

MASTER OF SCIENCE

IN

ELECTRICAL ENGINEERING

KING FAHD UNIVERSITY
OF PETROLEUM AND MINERALS

Dhahran, Saudi Arabia

May 2000

UMI Number: 1403698

Bell & Howell Information and Learning Company
300 North Zeeb Road
P.O. Box 1346
Ann Arbor, MI 48106-1346

KING FAHD UNIVERSITY OF PETROLEUM AND MINERALS

DHAHRAN 31261, SAUDI ARABIA

DEANSHIP OF GRADUATE STUDIES

This thesis, written by

SHAIKH HASIBUL MAJID

under the direction of his Thesis Advisor and approved by his Thesis Committee, has been presented to and accepted by the Dean of Graduate Studies, in partial fulfillment of the requirements for the degree of

MASTER OF SCIENCE IN ELECTRICAL ENGINEERING

Thesis Committee

Dr. M. M. Shahidul Hassan (Chairman)

Dr. Muhammad Taher Abuelma'ati (Member)

Dr. Abdul Kadir Hamid (Member)

Dr. Samir Al – Baiyat
(*Department Chairman*)

Prof. Osama A. Jannadi
(*Dean, College of Graduate Studies*)

13/11/2000
Date

Dedicated to

my loving parents,

Arch. Shaikh Abdul Mazid and *Mrs. Hosne Ara Begum.*

Acknowledgements

In the name of Allah, The Beneficent, The Merciful

All praise and glory be to Almighty Allah (SWT) who gave me courage and patience to carry out this work and peace and blessings of Allah (SWT) be upon Prophet Muhammad (SM).

My deep appreciation goes to my thesis advisor Dr. Mirza Mohammad Shahidul Hassan, for his constant help, guidance and the countless hours of attention those he devoted throughout the research work. Put in simple words, he has been an ideal advisor. It was because of him that the work at any point of time, never got stressed on me. Each time I went to meet him for the most trivial of problems, he was always kind, understanding and sympathetic to me.

Thanks are also due to my thesis committee members Professor Muhammad Taher Abu El Ma'ati and Dr. Abdul Kadir Hamid for their interest, cooperation, advice and constructive criticism. My learned committee was a pleasure to work with.

Acknowledgement is due to King Fahd University of Petroleum and Minerals for providing support for this research. Appreciation is due specially to Library facility. I also would like to acknowledge the Department of Electrical Engineering for providing me all types of supports during my stay here as a Graduate Student.

My family, specially my most loving Abba, Ma and sister, were a constant source of motivation. Their love carried me through some difficult moments.

Finally I would like to convey my special thanks to my colleagues and friends of KFUPM for their help and encouragement. It is worth to name a few like Mr. M. Mozahar Hossain, Mr. M. A. Rakib, Mr. Mohammad Nuruzzaman, Dr. Mohammad Niaz and Dr. Abu Nasser Khondaker. They have made my stay at KFUPM a very pleasant and unforgettable experience.

Contents

List of Tables

List of Figures

Nomenclature

A	Area of the Schottky contact (cm^2)
A^*	Effective Richardson constant (A/cm^2K^2)
C_j	Junction capacitance per unit area
D_p	Diffusion coefficient of hole (cm^2/s)
D_n	Diffusion coefficient of electron (cm^2/s)
E	Electric field (V/cm)
E_c	Energy of the conduction band (eV)
E_F	Energy of the Fermi level (eV)
E_v	Energy of the valance band (eV)
h	Plank's constant
J	Total current density (A/cm^2)
J_n	Electron current density (A/cm^2)

J_{ns}	Saturated electron current density (A/cm^2)
J_p	Hole current density (A/cm^2)
J_{pL}	Hole current density at the low-high interface (A/cm^2)
J_{pR}	Recombination current density within the drift region (A/cm^2)
J_r	Reverse current density (A/cm^2)
k	Boltzman's constant
L_a	Ambipolar diffusion length (cm)
L_d	Length of the drift region (cm)
m^*	Effective mass of Electron
n	Electron concentration (cm^{-3})
n^-	Lightly doped n type drift region
n^+	Heavily doped n type substrate
N_D	Density of donor impurity (cm^{-3})
N_A	Density of acceptor impurity (cm^{-3})
N_c	Number of effective density of states
p	Hole concentration (cm^{-3})
p_L	Hole concentration at the low-high interface (cm^{-3})
p_o	Hole concentration at the edge of the semiconductor side of the depletion region (cm^{-3})
q	Electric charge (C)

Q_s	Stored charge (C/cm^2)
R_{sub}	Substrate resistance ($\Omega - cm^2$)
S_{eff}	Effective surface recombination velocity (cm/s)
T	Temperature (K)
U_n	Electron recombination rate
U_p	Hole recombination rate
$\bar{v}$	Average thermal velocity of electrons (cm/sec)
V_a	Applied forward voltage (V)
V_i	Built-in voltage (V)
V_{inj}	Voltage across the drift region (V)
V_s	Voltage across the junction (V)
V_T	Thermal voltage (V)

μ_n	Electron mobility ($cm^2/V.s$)
μ_p	Hole mobility ($cm^2/V.s$)
τ_n	Electron lifetime (s)
τ_p	Hole lifetime (s)
τ_s	Storage time (s)
ϕ_i	Built in potential (V)
ϕ_m	Work function of the metal (V)

ϕ_s	Work function of the semiconductor (V)
ϕ_B	Barrier height (V)
χ_s	Electron affinity of the semiconductor (V)

THESIS ABSTRACT

Name: SHAIKH HASIBUL MAJID

Title: MINORITY CARRIER INJECTION IN EPITAXIAL SCHOTTKY BARRIER DIODES

Degree: MASTER OF SCIENCE
Major Field: ELECTRICAL ENGINEERING
Date of Degree: May, 2000

Lightly doped semiconductor region of an epitaxial Schottky Barrier (SB) diode is capable of sustaining large reverse voltage. To fabricate such SB diodes, higher resistivity and thicker layers are needed. The high resistance has detrimental effect on the performance of SB diode. The resistance can be reduced by minority carrier injection. An SB diode with higher barrier height injects an appreciable amount of minority carriers at low forward bias voltage. The J-V characteristic of an SB diode with injection of minority carriers are significantly altered from the classical exponential relationship. To analyze the different characteristics of an SB diode a model incorporating drift, diffusion currents, recombination and blocking properties of the low-high (n^-n^+) interface is developed. At low level of injection the J-V follows classical relationship. A significant deviation in J-V characteristic from its exponential behaviour occurs at high level of injection. The current is found to be strongly dependent on the width of the drift region and effective surface recombination velocity whereas, dependence on the doping density is not significant. The injection ratio and storage time are also found strongly dependent on L_d and S_{eff}. The low storage time can be achieved if the effective surface velocity is high; and stored charge is reduced if the thickness of the drift region is small.

Master of Science Degree
King Fahd University of Petroleum and Minerals
Dhahran, Saudi Arabia
MAY 2000

ملخص الرسالة

الاسم : شيخ حسيب مجيد

العنوان : حقن حوامل الشحنات الأقلية في ثنائيات (حاجز شوتكي) المستنبطة بطريقة "ايتاكس".

الدرجة : ماجستير

التخصص: الهندسة الكهربائية

التاريخ : مايو ٢٠٠٠م

من المعروف أن المناطق شبه الموصلة في ثنائي حاجز شوتكي المستنبط بطريقته ايتاكس تتحمل درجات عالية من فرق الجهد العكسي. وحتى يمكن تصنيع هذا النوع من الثنائيات لا بد من وجود طبقات سميكة ذات مقاومة عالية. هذه المقاومات العالية لها تأثير ضار على خصائص الثنائيات ومن الممكن إنقاص المقاومة بواسطة حقن حوامل شحنات الأقلية.

إن ثنائي حاجز شوتكي ذو الحاجز المرتفع بإمكانه حقن كمية لا بأس بها من حوامل شحنات الأقلية إذا تعرض لجهد تهيئة طبيعية . إن منحنى العلاقة بين فرق الجهد والتيار في ثنائي حاجز شوتكي يختلف اختلافا ملحوظا عن العلاقة الآسية التقليدية وذلك إذا تم حقنه بحوامل شحنات الأقلية. وتهدف هذه الأطروحة إلى تحليل الخصائص المختلفة لثنائي حاجز شوتكي وذلك باستنباط نموذج يمثل تيارات الاندفاع والانتشار وإعادة الاتحاد بين الشحنات وكذلك خصائص المعوقات الناتجة من السطح البيني الفاصل بين الطبقات ذات الشحنات الكثيفة والأخرى ذات الشحنات القليلة. وقد وجد انه إذا كان الحقن قليل فان منحنى العلاقة بين الجهد والتيار يظل كما هو في الحالة التقليدية. أما في حالة الحقن الكثيف فان هذا المنحنى يختلف اختلافا ملحوظا عن الشكل الأسي التقليدي. وقد وجد أن التيار يعتمد اعتمادا كبيرا على عرض طبقة الاندفاع وكذلك السرعة الفعلية لعودة الشحنات للاتحاد على السطح. أما الاعتماد على كثافة المعالجة فقد وجد ان تأثيره غير ملحوظ. وقد لوحظ أيضا إن نسبة الحقن وزمن التخزين تعتمد اعتمادا كبيرا على طول منطقة الاندفاع وكذلك سرعة إعادة اتحاد الشحنات على السطح. ويمكن الحصول على زمن تخزين قصير إذا كانت سرعة إعادة اتحاد الشحنات على السطح كبيرة وكذلك فان الشحنات المخزونة تقل إذا قل سمك منطقة الاندفاع.

درجة الماجستير في العلوم

جامعة الملك فهد للبترول والمعادن

مايو ٢٠٠٠م

Chapter 1

INTRODUCTION

1.1 Historical Background

Most of the electronic devices that make up an integrated circuit are connected by means of metal-semiconductor contacts. The earliest systematic investigation on metal-semiconductor rectifying systems is generally attributed to Braun [21],who in 1874 noted the dependence of the total resistance on the polarity of the applied voltage and on the detailed surface conditions. The point-contact rectifier in various forms found practical applications beginning in 1904 [21]. Wilson formulated the transport theory of semiconductors based on the band theory of solids in 1931 [22]. This theory was then applied to the metal-semiconductor contacts. In 1938 Schottky suggested that the potential barrier could arise from stable space charges in the semiconductor alone without the presence of a chemical layer. The model arising

from this consideration is known as the Schottky barrier (SB) [21].

This Barrier has found many applications in electronics. Specially the need for efficient and fast rectifiers and switches for their applications in power supplies for computers and office equipment for automotive industries. Even the high speed devices such as microwave mixers, high-frequency detectors and fast recovery rectifiers this SB diodes are used [1].

The application of an SB diode as a high speed device requires a small value of its capacitance. The capacitance of an SB is smaller than that of its counter part, pn junction device. The junction capacitance (per unit capacitance)of an SB is given by [17]:

$$C_j(SB) = \left[\frac{q\epsilon_s N_D}{2(\phi_i - V_a))}\right]^{\frac{1}{2}} \tag{1.1}$$

where C_j is the capacitance per unit area for finite values of N_D.

There is another type of capacitance which is called diffusion capacitance. Diffusion capacitance represents the capacitance associated with incremental changes in the injected minority-carrier charge. When pn junction is forward biased electrons are injected into the p side and holes are injected into the n side of the junction. The analog of electron minority-carrier storage in p side of pn junction with SB diode made from n type semiconductor is the storage of electrons after they have been injected into the metal. Metal acts as a source of of electrons. The injected electrons cannot produce an effect on the total number of electrons. Therefore, there is no direct analog of minority carrier storage in an SB diode.

On the other hand, that for SB with higher barrier height, the effect of the minority carrier holes injected into n-semiconductor cannot be neglected, which is direct analog of minority carrier holes in pn junction. As the storage of minority carrier electrons in metal of an SB is neglected, the capacitance of a forward-biased SB diode is smaller than that of a pn junction with same N_D. The capacitance controls the time constant of a device. The time constant is small when the capacitance of the device is small. A small time constant is desired to use the device for switching purpose. An SB has advantage over pn diode in this respect.

1.2 Schottky barrier

When a metal and Si-semiconductor forms a contact depending upon their work functions this can be an ohmic contact or a rectifying contact. Sometimes the contact itself offers negligible resistance to current flow compared to its bulk resistance. This contact allows the current to flow both in reverse bias and forward bias condition. The rectifying contact is called as Schottky Barrier (SB). The SB contact allows current to flow only in forward bias condition.

The energy band diagram in Figure 1.1 and Figure 1.2 illustrate the process of barrier formation. Figure 1.1 shows the electron energy band diagram of a metal of work function ϕ_m and an n-type semiconductor of work function ϕ_s which is smaller than ϕ_m. The work function ϕ_s of the semiconductor is defined as a variable quantity

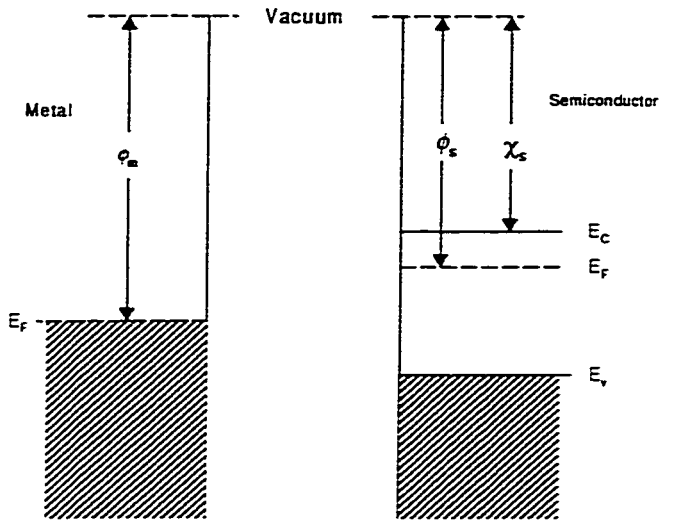

Figure 1.1: Energy levels for metal and semiconductor, when they are apart from each other [17]

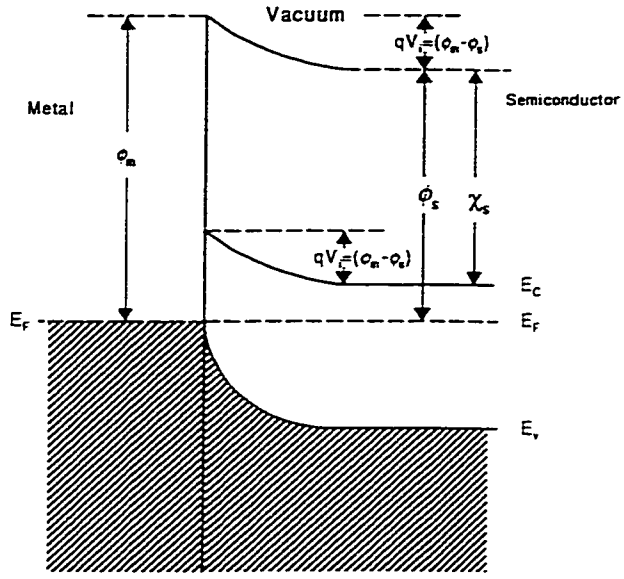

Figure 1.2: Metal and semiconductor contact band-diagram [17]

because the Fermi level in the semiconductor varies with the doping. An important surface parameter which does not depend on doping is the electron affinity χ_s defined as the energy difference of an electron between the vacuum level and the lower edge of the conduction band. Figure 1.2 shows the band diagram of a metal-semiconductor at the thermal equilibrium.

In a metal-semiconductor junction the difference between the work function of the metal ϕ_m and the electron affinity χ_s of an n-type semiconductor, shown in Figure 1.1, determines the barrier height (ϕ_B=ϕ_m-χ_s) for the model shown in Figure 1.2. The barrier forms by equalization of the Fermi levels across the junction due to the movement of electrons from the semiconductor to the metal interface. The barrier in the semiconductor itself is $qV_i = (\phi_m - \phi_s)$. The barrier exists only when $\phi_m > \phi_s$.

The ohmic metal-semiconductor contact shows a linear I-V characteristics in both biasing directions. Ideal Metal-semiconductor contacts are ohmic when the charge induced in the semiconductor in aligning the Fermi levels is provided by majority carriers shown in Figure 1.3. In n-type and in $\phi_m < \phi_s$ case of Figure 1.3, the Fermi levels are aligned at equilibrium by transferring electrons from the metal to the semiconductor. This raises the semiconductor electron energies relative to the metal at equilibrium Figure 1.3(b). In this case the barrier to electron flow between the metal and the semiconductor is small and easily overcome by a small voltage [20].

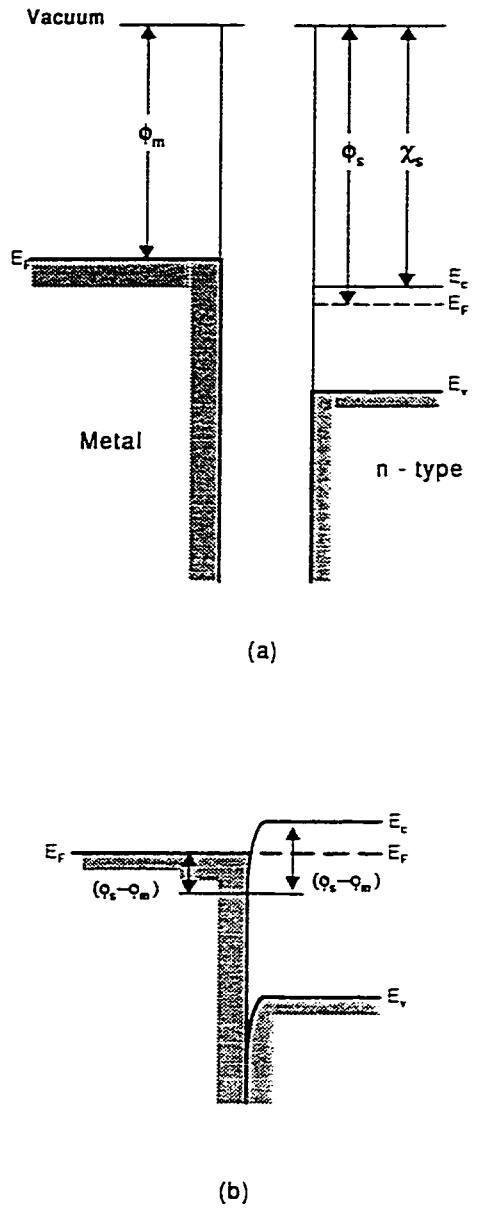

Figure 1.3: Ohmic metal-semiconductor contact (a)For n-type semiconductor, and (b) The equilibrium band diagram for the junction [20]

An electron emitted over the barrier from semiconductor into the metal must move through the high field depletion region. In traversing this region the motion of the electron is governed by the drift and the diffusion process and the emission of electrons into the metal is controlled by the density of available states in the metal. Thus the three processes

i. Drift

ii. Diffusion and

iii. Recombination

are the controlling parameters of current. According to Bethe [3, 17], the diode current is limited by thermionic emission over the barrier. This thermionic drift diffusion theory is described in the following section:

1.2.1 Thermionic Emission-Diffusion theory

The effect of drift and diffusion in the depletion region is assumed to be negligible in this theory. The barrier height is assumed to be large compared to kT. Only those electrons who has achieved a kinetic energy more than the height of the potential barrier ϕ_B will be able to reach the top of the barrier. Assuming that the electrons have a Maxwellian distribution of velocities, the number of electrons having sufficient energy to cross the barrier [17],

$$n* = n_o exp\left[\frac{-q(V_i - V)}{kT}\right] \tag{1.2}$$

where, V is the applied bias voltage and n_o represents the number of electron concentration in the neutral semiconductor and is expressed by,

$$n_o = N_c exp(-\frac{\phi_n}{kT}) \tag{1.3}$$

where $\phi_B = qV_i + \phi_n$ and $\phi_n = E_c - E_F$. From equation 1.2 the following equation is obtained:

$$n* = N_D exp\left[-\frac{(\phi_B - qV)}{kT}\right] \tag{1.4}$$

By assuming that there is no reflection of electron the following expression for electron current from semiconductor to metal is obtained [17]:

$$I_{SM} = \frac{qA\bar{v}}{4} N_D exp\left[-\frac{(\phi_B - qV)}{kT}\right] \tag{1.5}$$

For unbiased junction net current flow must be zero. Therefore, current flowing from metal to semiconductor is [17]:

$$I_{MS} = -\frac{qA\bar{v}}{4} N_D exp\left[-\frac{(\phi_B)}{kT}\right] \tag{1.6}$$

In the presence of an applied bias voltage V, $I_{MS} = -I_o$ and the following equation is obtained:

$$I = I_o\left[exp\left(\frac{qV}{kT}\right) - 1\right] \tag{1.7}$$

where, $\bar{v} = (8kT/\pi m^*)^{1/2}$ and $N_c = 2(2m^*kT/h^2)^{3/2}$ and I_o is as follows [17]:

$$I_o = AA^*T^2 exp\left(-\frac{\phi_B}{kT}\right) \tag{1.8}$$

where A is the area of the Schottky contact.

1.3 Review of previous works

Works on Schottky Barrier diode mainly studied the current-voltage characteristics, storage time and injection ratio of the diode. The minority carrier injection and charge storage in epitaxial Schottky-barrier diodes have been studied previously by a number of researchers.

The work in [16] considered the drift current. The analysis was restricted by the condition that the minority carrier concentration and current remained small compared to the majority carrier concentration and current. In his work the author has studied the minority carrier injection and charge storage in an epitaxial Schottky Barrier diode. Only drift current was considered in finding minority carrier profile. Recombination in the injection region was neglected.

Later C.T.Chung [4] carried out an analysis for minority carrier and charge storage considering both the drift and diffusion components of majority and minority currents. But the author did not include recombination current in obtaining an expression for minority carrier profile.

L. Stolt et al., [19] carried out numerical analysis for Schottky barrier (SB) on silicon using high barriers. For SB diodes with high breakdown voltage the semiconductor with higher resistivity and thicker layers is needed. For this structure the bulk resistance becomes substantial. However the authors have shown that the ohmic drop can be reduced by minority carrier injection. At high level of minority

carrier injection, the whole epitaxial layer will be conductivity modulated and as a result the ohmic drop could be reduced.

Some experimental works have been done on the current-voltage characteristics of SB diodes in [1, 2, 5, 6, 11, 15]. Experimental results show that the current increases with voltage. At low current densities, current exhibits exponential relationship with voltage and at a larger current densities the current does not follow the exponential relationship. It follows a relationship with voltage that can be approximated by a polynomial.

1.4 Objective of the thesis

Schottky diodes are used for low voltage rectification because of their advantage over pn-diodes is that they have relatively low forward voltage drop [19]. As they have low forward voltage drop, they possess low power dissipation. To get a high reverse breakdown voltage higher resistivity and thicker layers are needed. But due to the thick layer, bulk resistance becomes significant. This added resistance can be reduced by minority carrier injection for the case of SB diode.

The SB diode is a majority carrier device. But under high level of injection (with sufficiently large forward bias) the minority current injection ratio increases with current density due to the enhancement of drift-field component and the requirement of charge neutrality in the quasi-neutral region.

In previous works recombination of minority carrier current within the Si semiconductor was not included. Low injection and high injection were studied separately.

In this thesis the profile of minority carrier under low and high injection will be studied. In obtaining minority carrier profile both drift and diffusion currents and recombination of minority carrier are considered. An analytical expression valid for both regions of injection will be obtained using established relations derived for low and high injection.

The obtained expression for minority carrier within the semiconductor can be used in studying J-V characteristic of an SB diode both for low and high voltages. The storage time and injection ratio are also studied.

1.5 Summary of the thesis

In chapter 1 of this thesis, literature survey of SB diode will be undertaken. A brief description of theory for Schottky Barrier will be reviewed in this chapter.

In Chapter 2 mathematical analysis for determination of minority carrier profile, electric field distribution and voltages within the drift region for different level of injection of minority carriers is given. The minority carrier profile within the drift region is obtained considering the drift-diffusion current densities, recombination within the drift region and the blocking properties of minority carrier of low-high

(n^-n^+) junction.

Using the mathematical formulations derived in Chapter 2, the J-V characteristics, injection ratio and storage time are studied. All the relevant equations required for studying the characteristic of SB diode are derived using basic equations and with some assumptions in chapter 3. Chapter 4 contains the concluding remarks along with suggestions for future work on the topic.

Chapter 2

Analysis of drift region for different levels of Injection

2.1 Introduction

Schottky Barrier (SB) is basically a majority carrier device at low level of injection. The modern Schottky Barrier structures can withstand high reverse voltage. For these structures the bulk resistance becomes substantial. The ohmic drop across the semiconductor can be reduced by minority carrier injection. Which is the case of pn-diodes but not for normal SB diodes. The disadvantage of pn-diodes compared to Schottky diodes is that the former has a higher voltage drop across the junction. Minority crrier injection can be obtained in high barrier Schottky diodes. In the present work the characteristics of such diodes are investigated theoretically. In this

chapter the relevant equations, required for studying the characteristics of an SB diode, are derived.

The low-injection region of operation and high-injection region of operation are studied separately. In determining minority carrier profile for low level injection, drift and diffusion currents are taken into account. For high levels of injection, in addition to drift and diffusion currents the minority carrier recombination is incorporated. At high level of injection, the minority carriers invade the whole drift region. A large accumulation of minority and majority carriers will occur within the drift region. The minority charge stored in the drift region depends upon the characteristics of the epi-substrate interface and can become very significant. Therefore, the characteristics of the contact at the end need to be considered. The modern SB is of metal-n^-n^+ type. The n^-n^+ contact blocks the minority carriers [7]. The minority carrier reflecting properties of the epitaxial-substrate interface (n^-n^+) is taken into account in finding profile for the minority carriers.

2.2 Derivation of the equations

The structure of a SB diode, under the present study is shown in figure 2.1. Both sides of the Si-semiconductor is sandwiched by two metal contacts. The left metal-semiconductor junction forms the SB contact and the right one creates Ohmic contact. The drift layer considered here is made of lightly doped n-type semiconductor

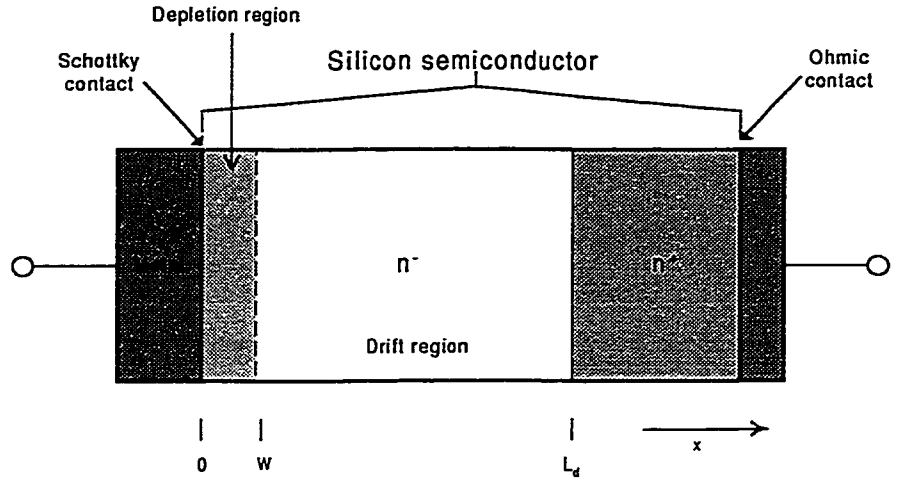

(a)

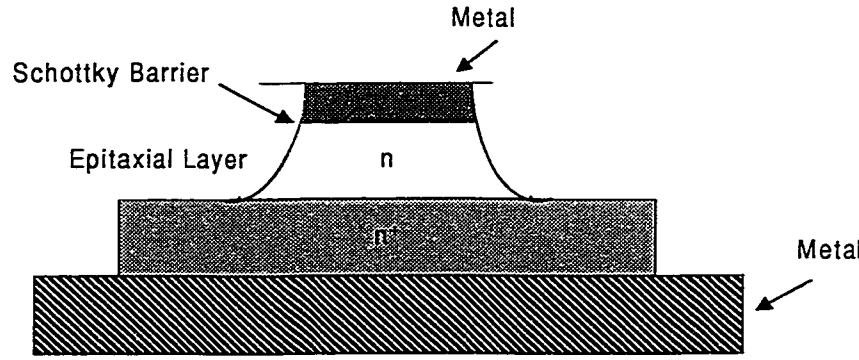

(b)

Figure 2.1: (a) Simplified structure of SB for analysis and (b) Schematic cross section of an SB diode [10].

of constant doping N_D bounded by a heavily doped n^+ region at a distance L_d.

When the SB is forward biased, holes are injected into the n-semiconductor. On the other hand, electrons move towards the SB contact leading to a quasi-neutral situation accompanying the hole pile up. The electron and hole distribution within the semiconductor can be obtained solving the drift-diffusion currents and continuity equations. .

2.2.1 Basic equations

The expression for minority carrier profile within the drift region can be obtained solving basic equations and applying the quasi-neutral condition. The basic equations are [12]:

$$J_n = q\mu_n n(x)E(x) + qD_n\frac{dn}{dx} \tag{2.1}$$

$$J_p = q\mu_p p(x)E(x) - qD_p\frac{dp}{dx} \tag{2.2}$$

$$\frac{1}{q}\frac{dJ_n}{dx} = \frac{n}{\tau_n} \tag{2.3}$$

$$\frac{1}{q}\frac{dJ_p}{dx} = -\frac{p}{\tau_p} \tag{2.4}$$

The quasi-neutrality condition [8] requires :

$$p - n + N_D = 0 \quad \text{when} \quad 0 < x \leq L_d - W \tag{2.5}$$

$$\frac{dp}{dx} = \frac{dn}{dx} \tag{2.6}$$

The equations 2.1, 2.2, 2.3 and 2.4 2.5 are used in finding p(x), n(x) and E(x) for different levels of injection.

2.2.2 High injection

At high level of injection, minority carrier holes pile up within the drift region to sustain the hole current and are almost completely neutralized by the electrons. The result creates a conductivity modulation region with a low and slowly varying electric field and drift-diffusion hole current. The drift region is thus conductivity modulated from x=W to x=L_d. Taking into account this hole current, total current density is given by:

$$J = J_p + J_n \tag{2.7}$$

where the total current density J is constant throughout the drift region.

Analysis for high injection condition can be carried out i. considering recombination within the drift region and ii. without recombination within the drift region.

A. With recombination within the drift region

Differentiating 2.1 and 2.2 with respect to x we get:

$$\frac{dJ_n}{dx} = q\mu_n E\frac{dn}{dx} + q\mu_n n\frac{dE}{dx} + qD_n\frac{d^2n}{dx^2} \tag{2.8}$$

$$\frac{dJ_p}{dx} = q\mu_p E\frac{dp}{dx} + q\mu_p p\frac{dE}{dx} - qD_p\frac{d^2p}{dx^2} \tag{2.9}$$

From 2.2 we get:

$$E(x) = \frac{J_p}{q\mu_p p(x)} + \frac{D_p}{\mu_p p(x)} \frac{dp(x)}{dx} \tag{2.10}$$

Using 2.1, 2.2 and 2.7 the following is obtained:

$$J = J_n + J_p = (q\mu_n n + q\mu_p p) \left[\frac{J_p}{q\mu_p p} + \frac{D_p}{\mu_p p} \frac{dp}{dx} \right] + qD_n \frac{dn}{dx} - qD_p \frac{dp}{dx} \tag{2.11}$$

For high injection $p >> N_D$ and equation 2.5 reduces to:

$$n = p \tag{2.12}$$

Using 2.12, equation 2.11 can be written as:

$$J = q\mu_n p \left(1 + \frac{\mu_p}{\mu_n}\right) \left[\frac{J_p}{q\mu_p p(x)} + \frac{D_p}{\mu_p p(x)} \frac{dp(x)}{dx} \right] + qD_n \left(1 - \frac{D_p}{D_n}\right) \tag{2.13}$$

Rearranging equation 2.13 the following expression is found:

$$J = \frac{(1+m)}{m} J_p + 2qD_n \frac{dp}{dx} \tag{2.14}$$

where $\frac{D_p}{\mu_p} = \frac{D_n}{\mu_n} = V_T$ and $m = \frac{\mu_p}{\mu_n} = \frac{D_p}{D_n}$.

Equation 2.14 can be written as:

$$\frac{dp}{dx} = \frac{mJ - (1+m)J_p}{2qD_p} \tag{2.15}$$

Differentiating both sides of 2.15 with respect to x:

$$\frac{dJ}{dx} = \frac{(1+m)}{m} \frac{dJ_p}{dx} + 2qD_n \frac{d^2p}{dx^2} \tag{2.16}$$

The total current J must be constant, which gives:

$$\frac{dJ}{dx} = 0 \tag{2.17}$$

Using 2.4, 2.16 and 2.17 the following second order differential equation is obtained:

$$\frac{d^2p}{dx^2} = \frac{p}{L_a^2} \tag{2.18}$$

where L_a is the ambipolar diffusion length and is given by:

$$L_a = \sqrt{\frac{2\tau_p D_p}{1+m}} \tag{2.19}$$

In obtaining 2.18 for high injection, $p \cong n \gg N_D$ and $\frac{dn}{dx} = \frac{dp}{dx}$ for constant N_D are used.

The minority carrier profile p(x) within the injection region considering recombination, drift and diffusion current densities is governed by a second order differential equation 2.18. The solution of the equation can be written in the following standard form [8]:

$$p(x) = C\cosh\frac{x}{L_a} + D\sinh\frac{x}{L_a} \tag{2.20}$$

where C and D are arbitrary constants. To evaluate the values for C and D two boundary conditions are required.

At x=W, $p(W) \approx p(0) = p_0$

assuming $W \approx 0$, where p_0 is the injected electron carrier density at the depletion edge. The above boundary condition gives $C = p_0$.

The second boundary condition is chosen at x=L_d. At x=L_d the hole current density is given by $J_p(x = L_d) = J_{pL}$. Replacing J_p in 2.15 by J_{pL}, 2.15 becomes:

$$\frac{dp}{dx}|_{x=L_d} = \frac{mJ - (1+m)J_{pL}}{2qD_p} \tag{2.21}$$

When the whole drift region is invaded by the minority carriers, the hole concentration at $x = L_d$ depends upon the effective surface recombination velocity S_{eff} at the edge of the low-high n^-n^+ junction [7]. The n^-n^+ junction acts as a barrier to the flow of minority carrier current from the low to the high region and the minority carrier current is proportional to the carrier density at the low high junction. The hole current density at the interface is given by:

$$J_{pL} = qS_{eff}p_L \tag{2.22}$$

where p_L is the hole density at distance L_d.

Replacing C by p_o in 2.20 the following equation can be obtained:

$$p_L = p_o \cosh\frac{L_d}{L_a} + B\sinh\frac{L_d}{L_a} \tag{2.23}$$

Using 2.20, 2.23 and 2.21 we obtain the value of D (Details shown in Appendix A), which is:

$$D = \frac{1}{R}\left[\frac{mJL_a}{2qD_p} - \frac{(1+m)L_aqS_{eff}p_o}{2Dp}\cosh\frac{L_d}{L_a} - p_o\sinh\frac{L_d}{L_a}\right] \tag{2.24}$$

where

$$R = \cosh\frac{L_d}{L_a} + \frac{(1+m)L_aS_{eff}}{2D_p}\sinh\frac{L_d}{L_a} \tag{2.25}$$

Substituting C and D in 2.20, the following equation of the hole concentration is obtained:

$$p(x) = p_o\cosh\frac{x}{L_a} + \frac{1}{R}\left[\frac{mJL_a}{2qD_p} - \frac{(1+m)L_aS_{eff}p_o}{2Dp}\cosh\frac{L_d}{L_a} - p_o\sinh\frac{L_d}{L_a}\right]\sinh\frac{x}{L_a} \tag{2.26}$$

Rearranging 2.26 we obtain the equation for p(x)(Appendix A):

$$p(x) = \frac{1}{R}\left[p_o \cosh\frac{L_d - x}{L_a} + \frac{p_o L_a (1+m) S_{eff}}{2D_p}\sinh\frac{L_d - x}{L_a} + \frac{mJL_a}{2qD_p}\sinh\frac{x}{L_a}\right] \tag{2.27}$$

To find the electric field E(x) 2.7, 2.1 and 2.2 are used. Using these equations the following expression for E(x) is found (Appendix B):

$$E(x) = \frac{J}{q\mu_n(1+m)}\frac{1}{p(x)} + V_T\frac{(1-m)}{(1+m)}\frac{1}{p(x)}\frac{dp}{dx} \tag{2.28}$$

The voltage across the injection region V_{inj} can be obtained by:

$$V_{inj} = -\int_0^{L_d} E(x)dx \tag{2.29}$$

The above equation can be written as (Appendix B):

$$V_{inj} = -\frac{JR}{q\mu_n p(1+m)\sqrt{b^2-a^2}}\ln\frac{\frac{a\tanh\frac{L_d}{2}+b-\sqrt{b^2-a^2}}{a\tanh\frac{L_d}{2}+b+\sqrt{b^2-a^2}}}{\frac{b-\sqrt{b^2-a^2}}{b-\sqrt{b^2+a^2}}} + V_T\frac{(1-m)}{(1+m)}\ln\frac{p_o}{p_L} \tag{2.30}$$

where

$$\begin{aligned} a &= p_o\cosh\frac{L_d}{L_a} + \frac{p_o L_a(1+m)}{2D_p}S_{eff}\sinh\frac{L_d}{L_a} \\ b &= \frac{mJL_a}{2qD_p} - p_o\sinh\frac{L_d}{L_a} - \frac{p_o L_a(1+m)}{2D_p}S_{eff}\cosh\frac{L_d}{L_a} \end{aligned}$$

Equation 2.30 is valid for $a^2 < b^2$.

When $a^2 > b^2$ V_{inj} the integration gives:

$$V_{inj} = -\frac{JR}{q\mu_n p(1+m)\sqrt{b^2-a^2}}\frac{\arctan\frac{-a\tanh\frac{L_d}{2L_a}+b}{\sqrt{a^2-b^2}}}{\arctan\frac{b}{\sqrt{a^2-b^2}}} + V_T\frac{(1-m)}{(1+m)}\ln\frac{p_o}{p_L} \tag{2.31}$$

Substituting p(x) from 2.27 into 2.16, an expression for $J_p(x)$ can be obtained and is given by (Appendix C):

$$J_p(x) = \frac{mJ}{(1+m)} + \frac{2qD_p}{(1+m)RL_a} \left[p_o \sinh \frac{L_d - x}{L_a} + \frac{p_o(1+m)L_a S_{eff}}{2D_p} \cosh \frac{L_d - x}{L_a} - \frac{JL_a}{2qD_n} \cosh \frac{x}{L_a} \right] \quad (2.32)$$

The hole current entering the drift region through x=0 is denoted by J_{po}. An analytical expression of J_{po} can be easily obtained from 2.32 by putting x-0. Putting x=0 in 2.32 the following expression of J_{po} is obtained:

$$J_{po} = \frac{mJ}{(1+m)} + \frac{2qD_p}{(1+m)RL_a} \left[p_o \sinh \frac{L_d}{L_a} + \frac{p_o(1+m)L_a S_{eff}}{2D_p} \cosh \frac{L_d}{L_a} - \frac{JL_a}{2qD_n} \right] \quad (2.33)$$

All the equations required for studying the characteristics of SB diode at high injection are obtained above.

When the recombination current J_{pR} is much smaller than J_{pL}, the recombination current within the drift region can be neglected. The necessary condition is as follows (Details are shown in Appendix D) :

$$p_o \gg \frac{\frac{m(R-1)}{m+R} J_{no} - \frac{mJL_a S_{eff}}{RD_p} \sinh \frac{L_d}{L_a}}{\frac{2qS_{eff}}{R} - \frac{2qD_p}{(m+R)L_a} \left[1 + \frac{(1+m)L_a S_{eff}}{2D_p} \right] \sinh \frac{L_d}{L_a}} \quad (2.34)$$

B. Without recombination within the drift region

When recombination within the drift region is neglected, the hole current J_p flowing through the drift region will be constant.

Equations 2.1, 2.2 and 2.6 can be used to find an expression of p(x), E(x) and V_{inj}.

Equations 2.1 and 2.2 can be rearranged with the help of 2.6:

$$\begin{aligned} \frac{J_n}{q\mu_n} &= nE(x) + V_T\frac{dn}{dx} \\ &= nE(x) + V_T\frac{dp}{dx} \qquad (2.35) \\ \frac{J_p}{q\mu_p} &= pE(x) - V_T\frac{dp}{dx} \qquad (2.36) \end{aligned}$$

Adding 2.35 with 2.36 and rearrangement gives the following expression for E(x):

$$E(x) = \frac{1}{q\mu_p(2p(x) + N_D)}[J_p + mJ_n] \qquad (2.37)$$

Taking the value of E(x)from 2.37 and substituting this in 2.36, the following is obtained:

$$\frac{dp}{dx} = \frac{(mJ_n - J_p)p - J_pN_D}{qD_p(2p + N_D)} \qquad (2.38)$$

Equation 2.38 can now be written as:

$$\left[1 + \frac{\frac{N_D}{2}\frac{mJ_n+J_p}{mJ_n-J_p}}{p - \frac{J_pN_D}{mJ_n-J_p}}\right] dp = \frac{mJ_n - J_p}{2qD_p}dx \qquad (2.39)$$

Upon integration of right side of 2.38 from p_o to $p(x)$ and left side from 0 to x the following expression is found:

$$p(x) - p_o + \frac{N_D}{2}\frac{mJ_n + J_p}{mJ_n - J_p}\ln\frac{p(x) - \frac{J_pN_D}{mJ_n-J_p}}{p_o - \frac{J_pN_D}{mJ_n-J_p}} = \frac{mJ_n - J_p}{2qD_p}x \qquad (2.40)$$

The hole distribution within the drift region can be obtained if p_o, J_n and J_p are known.

Hole concentration at the low-high interface (n^-n^+) p_L is obtained using 2.40. Instead of integrating from 0 to x, the following expression for p_L is obtained by integrating 2.38 from 0 to L_d. The expression of p_L is:

$$p_L - p_o + \frac{N_D}{2}\frac{mJ_n + J_{pL}}{mJ_n - J_{pL}} \ln \frac{p_L - \frac{J_{pL}N_D}{mJ_n - J_{pL}}}{p_o - \frac{J_{pL}N_D}{mJ_n - J_{pL}}} = \frac{mJ_n - J_{pL}}{2qD_p} L_d \tag{2.41}$$

Using 2.37 and 2.40, the integration 2.29 gives (Appendix E):

$$V_{inj} = \frac{J_{pL} + mJ_{no}}{J_{pL} - mJ_{no}} V_T \ln \frac{p_L - \frac{J_{pL}N_D}{mJ_{no} - J_{pL}}}{p_o - \frac{J_{pL}N_D}{mJ_{no} - J_{pL}}} \tag{2.42}$$

When injected minority carriers is not high, the hole current J_p becomes very small and can be neglected in the analysis. The necessary condition is as follows (Details are shown in Appendix F) :

$$mJ_{no} > qS_{eff}\left(\frac{N_D}{p_o} + 1\right) p_L \tag{2.43}$$

2.2.3 Low injection

When the injected carrier density is much less than the equilibrium majority carrier density then this condition is known as Low injection. At this level of injection, minority carrier current within the drift region can safely be neglected. In previous work [16], the reflecting boundary condition is taken as an approximation for a low-high (n^-n^+) junction at low currents.

At low injection, recombination can be neglected and $J_p = 0$.

When $J_p = 0$, 2.2 can be written as:

$$E(x) = V_T \frac{1}{p(x)} \frac{dp}{dx} \tag{2.44}$$

From 2.1, 2.5, 2.6 and 2.7, it is found that:

$$\begin{aligned} J = J_n &= q\mu_n n(x)E(x) + qD_n \frac{dn}{dx} \\ &= q\mu_n [p(x) + N_D]E(x) + qD_n \frac{dp}{dx} \end{aligned} \tag{2.45}$$

Substituting E(x) in 2.45 from 2.44 the following expression can be obtained:

$$\frac{J}{qD_n} = \left(\frac{2p(x) + N_D}{p(x)} \right) \frac{dp}{dx} \tag{2.46}$$

To find the expression for the hole concentration p(x) within the drift region 2.46 is needed to be integrated as follows:

$$\int_0^x \frac{J}{qD_n} dx = \int_{p_o}^{p(x)} \left(\frac{2p(x) + N_D}{p(x)} \right) dp \tag{2.47}$$

which gives the following expression:

$$\frac{J}{qD_n} x = 2p(x) - 2p_o + N_D \ln \frac{p(x)}{p_o} \tag{2.48}$$

This is a well known equation for p(x) when SB operates at low injection [14]. Hole concentration p(x) within the drift region for low injection case can be obtained if J and p_o is known.

Differentiating 2.48, and using 2.44:

$$\frac{J}{qD_n} = 2\frac{dp(x)}{dx} + \frac{N_D}{V_T} E(x) \tag{2.49}$$

Replacing E(x) in equation 2.49 by equation 2.46 the electric field E(x) is expressed as:

$$E(x) = \frac{J}{q\mu_n}\left[\frac{1}{2p(x) + N_D}\right] \tag{2.50}$$

Equation 2.48 can be written in the following integral form (Appendix G):

$$2\int_{p_o}^{p_L} dp(x) = \frac{J}{qD_n}\int_0^{L_d} dx - \frac{N_D}{V_T}\int_0^{L_d} E(x)dx \tag{2.51}$$

From 2.50 and 2.51, voltage across the drift region is written as (Appendix G):

$$V_{inj} = \frac{V_T}{N_D}\left[2(p_L - p_o) - \frac{JL_d}{qD_n}\right] \tag{2.52}$$

2.2.4 Injection ratio

There are two important parameters that characterize the SB diode. One is known as i. Injection ratio and the other one is ii. Storage time.

The injection ratio is defined as the ratio of minority carrier current to the total current. It is given by:

$$\gamma = \frac{J_{po}}{J_{po} + J_{no}} = \frac{J_{po}}{J} \tag{2.53}$$

When recombination within the drift region is not neglected, injection ratio can be given by (Appendix H):

$$\gamma = \frac{mJ(R-1)}{(1+m)R} + \frac{2qD_p}{(1+m)RL_a}\left[p_o \sinh\frac{L_d}{L_a} + \frac{p_o(1+m)L_aS_{eff}}{2D_p}\cosh\frac{L_d}{L_a}\right] \tag{2.54}$$

The above equation can be obtained from 2.33 and 2.53.

When recombination inside the drift region is neglected, J_{po} is constant. Then γ can be written as:

$$\gamma = \frac{J_{po}}{J} = \frac{J_{pL}}{J} \tag{2.55}$$

2.2.5 Storage time

For Schottky Barrier diode, the minority carrier stored charge per unit area (Q_s) depends upon the characteristics of the epitaxi-substrate interface and can become very significant when the interface is highly reflecting. Highly reflecting interface denotes that kind of interface which has a low value of surface recombination velocity (S_{eff}). The minority carrier stored charge per unit area can be derived using the following equation:

$$Q_s = q \int_0^{L_d} p(x)dx \tag{2.56}$$

The storage time τ_s can be derived by dividing the stored charge (Q_s) by the reverse current density J_r. Therefore, the equation for τ_s becomes as follows:

$$\tau_s = \frac{Q_s}{J_r} \tag{2.57}$$

2.2.5.1 High injection

A. With recombination within drift region

To find out the stored charge per unit area for the high injection case (with recombination), equations 2.27 and 2.56 are used. Taking the expression of p(x) from 2.27

into 2.56 the following expression for the stored charge per unit area (Q_s) for high injection is found:

$$Q_s = \frac{2\tau_p}{R}\left[\frac{mJ}{(1+m)} + qp_oS_{eff}\right]\sinh\frac{{L_d}^2}{2L_a} + \frac{p_oL_a}{R}\sinh\frac{L_d}{L_a} \tag{2.58}$$

Substituting Q_s in equation 2.57, τ_s can be obtained.

B. Without recombination within drift region

When the recombination within the drift region is neglected the stored charge per unit area is derived using 2.38 and 2.56. The expression becomes:

$$Q_s = \frac{2q^2D_p(p_L - p_o)(p_L + p_o - N_D) + qJ_pN_DL_d}{mJ_n - J_p} \tag{2.59}$$

Knowing Q_s, τ_s can be determined from equation 2.57.

2.2.5.1 Low injection

For low-injection, the stored charge per unit area Q_s is derived using 2.46 and 2.56. The equation is obtained as follows:

$$Q_s = \frac{q^2D_n}{J}(p_L - p_o)(p_L + p_o + N_D) \tag{2.60}$$

Using equation 2.60 and 2.57, storage time τ_s can be obtained.

2.3 Conclusion

All the equations required for studying the characteristics of a Schottky Barrier Diode are derived in this chapter. At high level of injection, the minority carrier

profile p(x) is obtained by solving a second order differential equation. To obtain a second order differential equation which is analytically tractable, two assumptions have been taken into account. i. Charge neutrality $p-n+N_D=0$ and ii. $p \approx n$. These two assumptions are widely used in analytical works for semiconductor devices. The profile p(x) for low-level injection is obtained considering zero recombination within the drift region and a perfectly reflecting low-high ($n^- n^+$) interface.

Chapter 3

RESULT AND DISCUSSION

3.1 Introduction

The characteristics of SB diode under different levels of injection are studied. In chapter 2, the equations for finding the minority carrier distribution within the drift region p(x), the electric field distribution E(x), minority carrier current density $J_p(x)$, injection ratio and storage time are obtained. For the high injection region, two different models, Model I and Model II have been established. Model I is for that level of high injection where recombination within the drift region has to be considered and Model II is that level of high injection where the recombination within the drift region is neglected. Computer programs are developed for generating different characteristic curves.

3.2 Illustration

In this thesis we mainly have studied an SB diode with high barrier height. When the barrier height is low then the SB is called a majority carrier device and the total current for SB with n-type semiconductor is contributed by electron current and hole current. At low level of injection electrons contribute the total current for both types of SB diode. The JV characteristics can be studied using low injection model. The JV characteristics with two different barrier heights are shown in Figure 3.1. The figure shows that cut in voltage for $\phi_B = 0.75$ is around 0.2 volts. On the other hand the cut in voltage becomes 0.35 for $\phi_B = 0.95$. This difference in cut in voltage is due to the ϕ_B. The saturation current J_{ns}, shown in equation 1.8 as J_o is given by [17]. Therefore, for a given current a higher applied voltage is required when ϕ_B is higher. From equation 1.7 we can say that for a constant current density higher applied voltage is required for higher barrier height.

For studying the behavior of SB diode under different levels of injection, the following have been used in computational work.

For computational work standard data for SB are taken, which are provided in the following tables Table 3.1 and Table 3.2 .

The hole concentration at x=0 (Fig. 2.1) is found by the following expression [16]:

$$p_o = \frac{N_D}{2}\left[\sqrt{1 + \frac{4n_i^2\left(\frac{J_{nc}}{J_{ns}} + 1\right)}{N_D^2}} - 1\right] \tag{3.1}$$

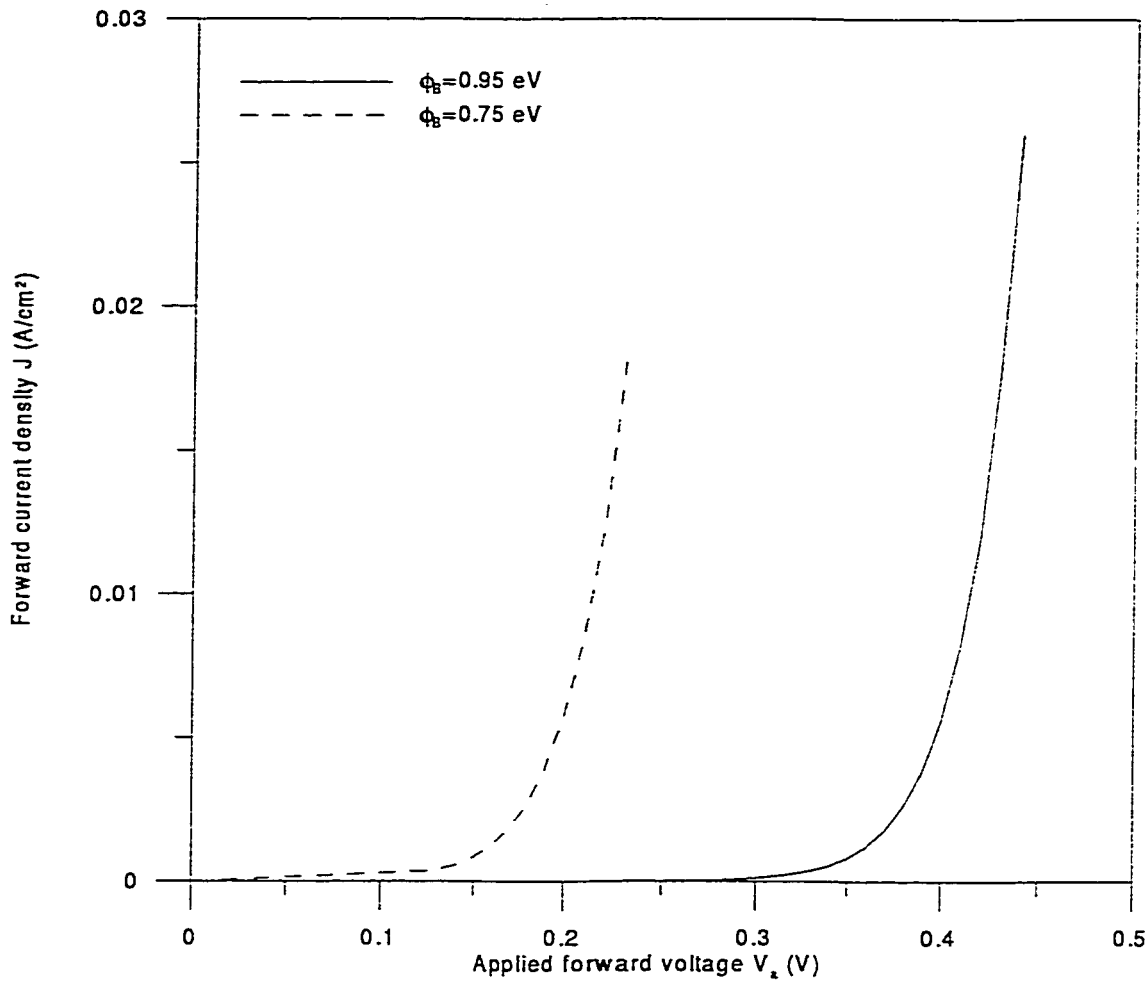

Figure 3.1: JV characteristics of an SB diode with different barrier height.

N_D cm^{-3}	L_d cm	S_{eff} cm/s
1×10^{15}	40×10^{-4}	1000

Table 3.1: Device parameters

D_p (cm^2/sec)	D_n (cm^2/sec)	J_{ns} (A/cm^2)	μ_p $(cm^2/V-sec)$	μ_n $(cm^2/V-sec)$	τ_p (μsec)
11.9084	34.4812	5×10^{-10}	459.78	1131.32	1

Table 3.2: Device make-up

The mobility μ_p and μ_n have been calculated from the relation given by Arora [9]:

The minority carrier lifetime is obtained from Y. P. Pai and H. C. Lin from [15] and is given by:

$$\tau_p = \frac{2 \times 10^{-6}}{1 + \frac{N_D}{10^{15}}} \tag{3.2}$$

The majority carrier current density J_{no}, flowing through the drift region of SB diode, is given by [13]:

$$J_{no} = J_{ns}\left[e^{\frac{V_s}{V_T}} - 1\right] \tag{3.3}$$

The diffusion coefficient in the n-semiconductor is given in [21] and can be expressed as:

$$\frac{D_p}{\mu_p} = \frac{D_n}{\mu_n} = V_T \tag{3.4}$$

3.3 Minority carrier distribution within the drift region

The hole distribution within the drift region of an SB diode for three different values of V_s is shown in Figure 3.2. The hole concentration at x=0 is p_o and is a function of V_s. This p_o is determined from equation 3.1. The regions of operation can be obtained from the boundary conditions 2.34 and 2.43. It is found that profile for hole concentration can be obtained using Model I for $V_s = .85V$ while for $V_s = .72V$ Model II can be used. Hole distribution under low injection condition is plotted for $V_s = .5V$.

Finding p(x) for Model I and Model II $S_{eff} = 1000$ is considered. On the other hand, for low injection perfect reflecting interface is assumed.

When recombination is occurred within the drift region, hole current density $J_p(x)$ decreases with increase of x due to loss of holes. As the n^-n^+ interface is not transparent to holes, holes are piled up near the interface and as a result p(x) increases with the increment of x.

When V_s is large, p_o is also large. At small V_s, p_o is small. Therefore, p(x) for Model I must be higher than that for Model II and also for low-injection.

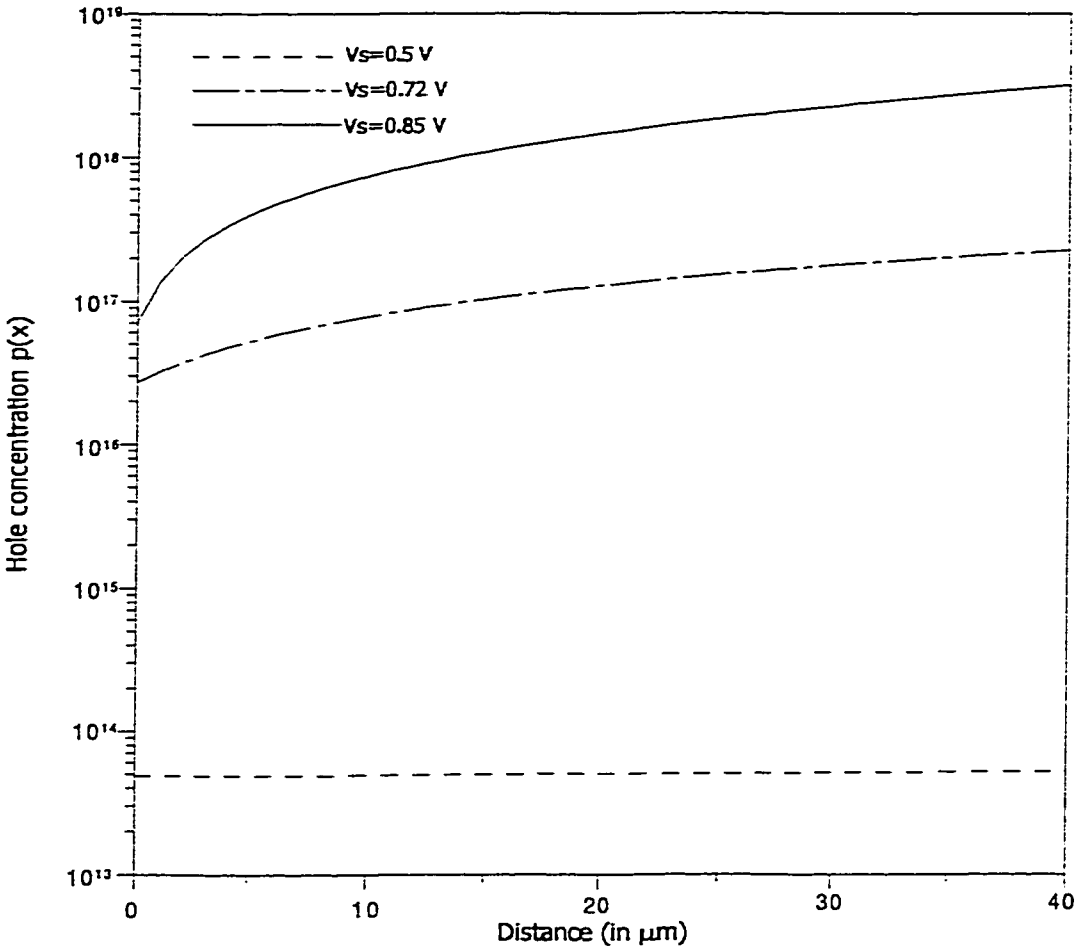

Figure 3.2: Minority carrier distribution within the drift region.

3.4 Electric field distribution within the drift region

Distribution of electric fields E(x) as a function of x is shown in the plot of Figure 3.3. In this Figure 3.3 the electric field is plotted for all three different regions of operation. The electric field E(x) decreases with the increment of x. Figure 3.2 shows that p(x) increases with x for all three regions of operation. The pile up of holes and electrons to maintain charge neutrality create a conductivity modulating zone within the drift region. Holes and electrons suppresses the electric field and the field will not be able to increase with the increment of x. For Model I and Model II, in Figure 3.2 it is found that the increment of hole density is much higher at the beginning than that of at the end. Similarly in Figure 3.3 the decrease of electric field is also much higher at the beginning. For low-injection model in Figure 3.2 the increase of holes is not that much significant which is also reflected in the electric field for low-injection in Figure 3.3.

3.5 Effect of the width of drift region on minority carrier concentration

Hole concentration for different widths of the drift region has been plotted in Figure 3.4. The plot shows that hole concentration profile goes up with the increment of

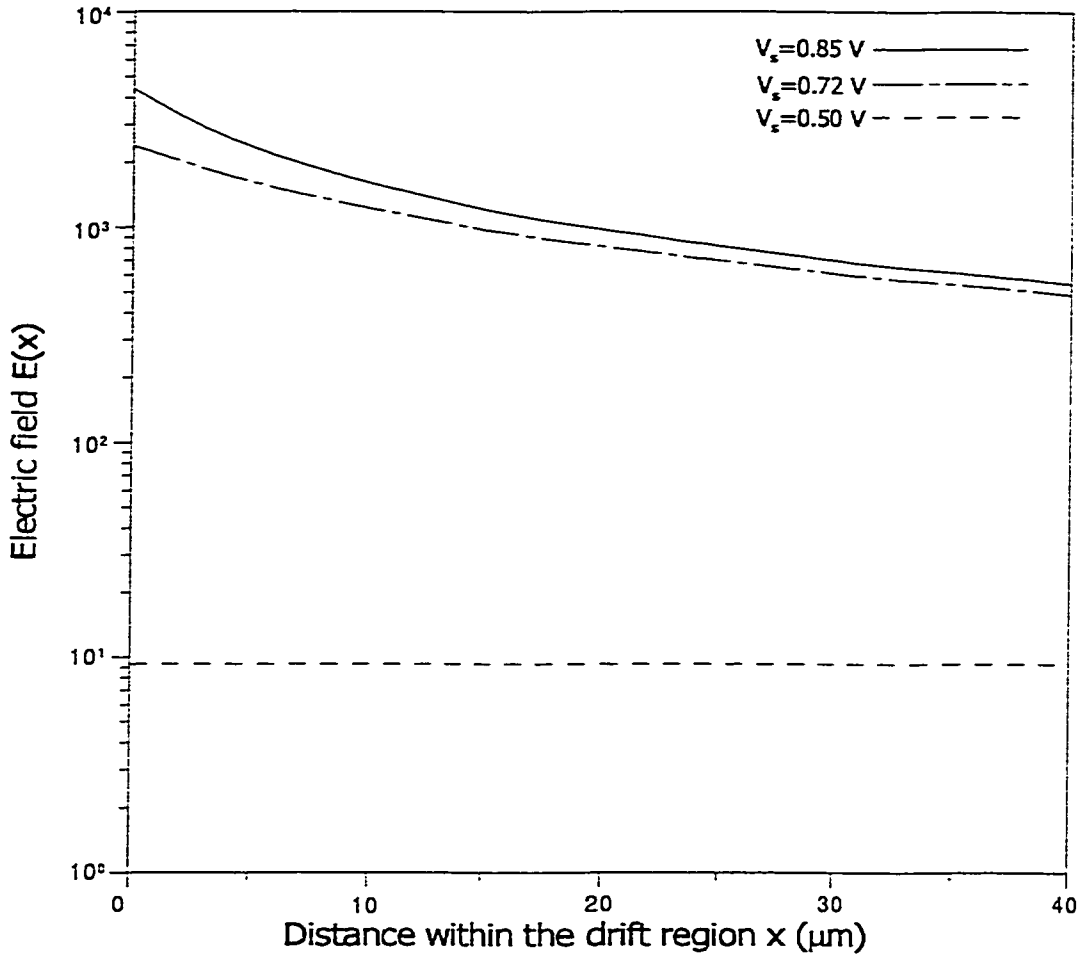

Figure 3.3: Electric field distribution within the drift region.

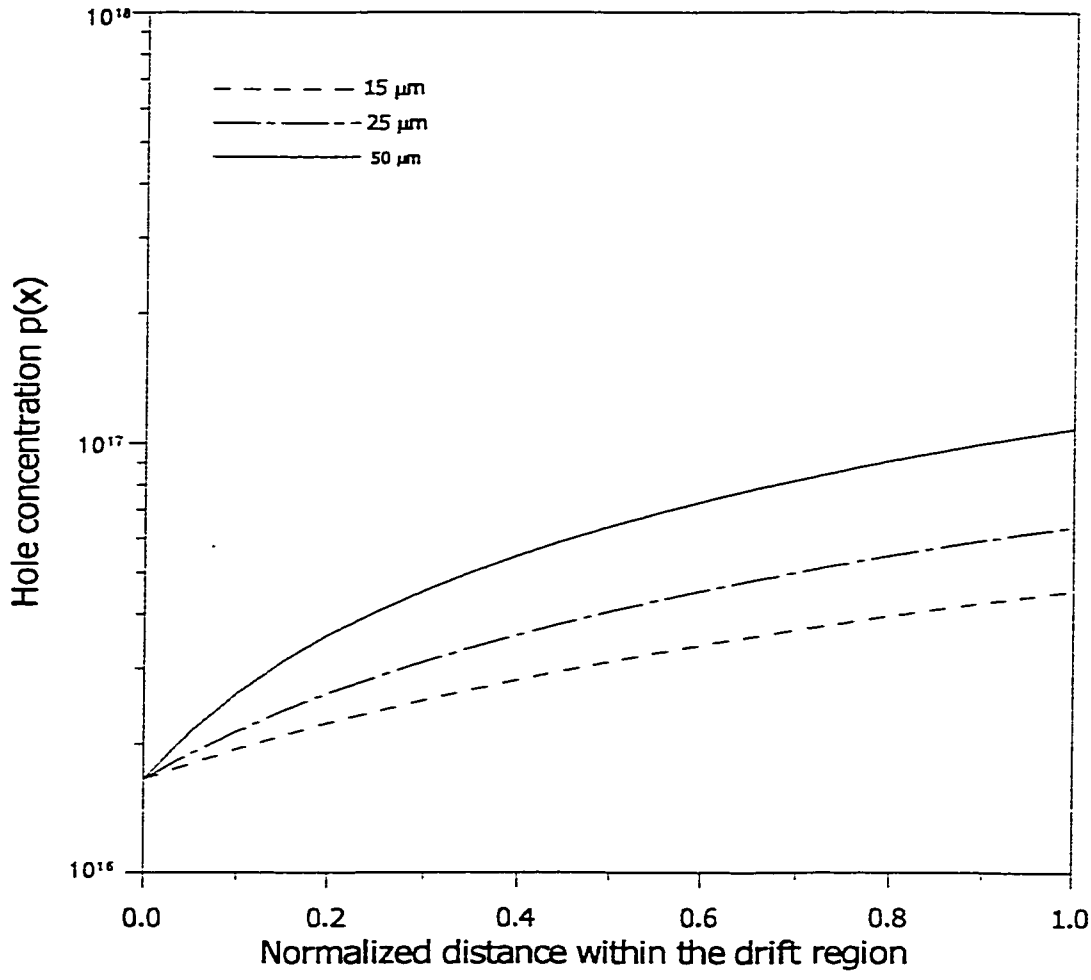

Figure 3.4: Effect of width of the drift region on hole concentration.

the length of the drift region. The plot has been done for $V_s = 0.725V$,the hole concentration at the edge of the depletion region p_o is same for the three curves. The hole recombination current density J_{pR} increases with the length of the drift region. Therefore the total hole current density J_p will be increased resulting an increase of holes.

3.6 Dependence of hole currents on the width of the drift region

Dependence of J_{po}, J_{pR} and J_{pL} on L_d is shown in Figure 3.5. For a given $V_s = 0.725V$, J_{po}, J_{pR} and J_{pL} are found to be increasing with L_d. When L_d is small, J_{pR} is insignificant. At a large L_d, J_{pR} is not small and exceeds J_{pL}. For a small SB diode, the recombination can be neglected and the characteristics can be studied using Model II and low-injection model. But for a large device, J_{pR} cannot be neglected. Model I, Model II and low-injection model are to be used to find the characteristics of an SB diode.

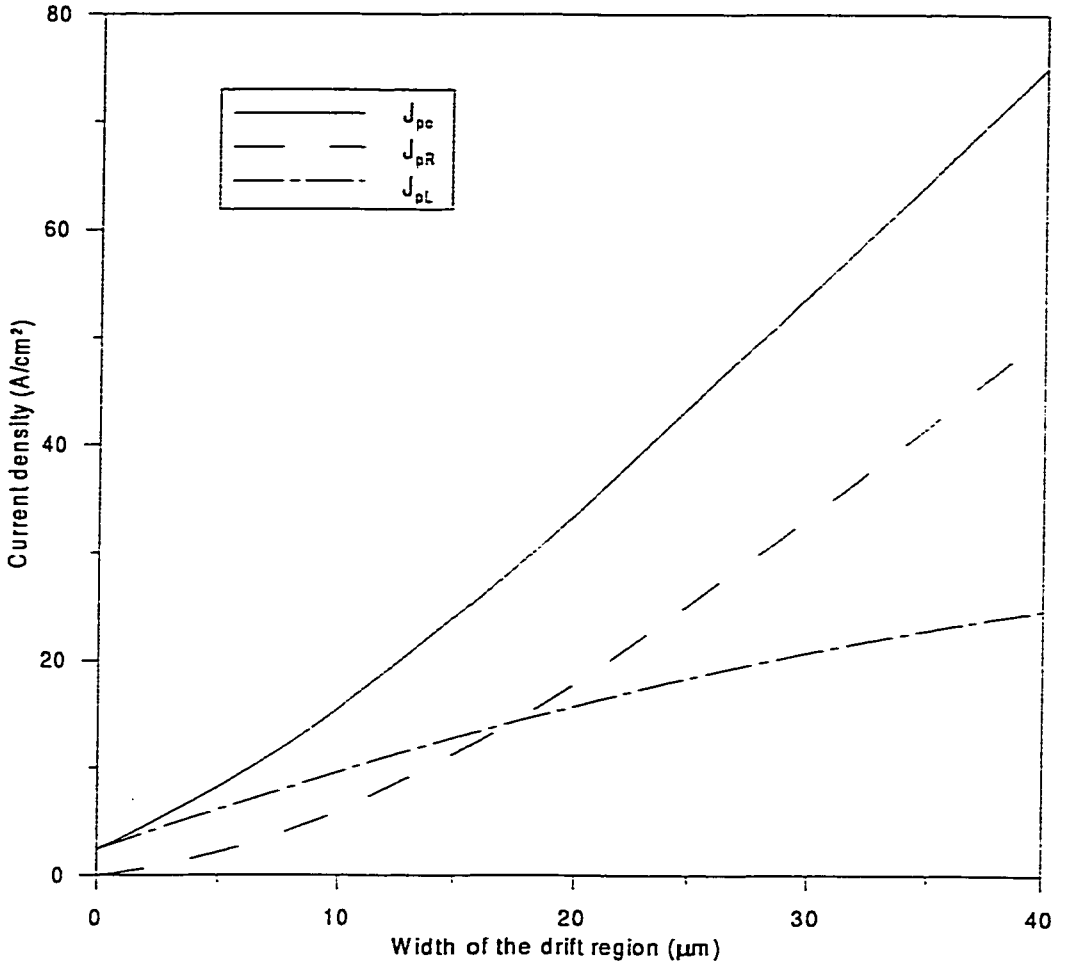

Figure 3.5: Effect of width of the drift region on minority carrier currents.

3.7 Effect of effective surface recombination velocity S_{eff} on carrier profile

Figure 3.6 shows the p(x) as a function of the distance x for three different values of S_{eff}. To plot this curve $S_{eff} = 10^3, S_{eff} = 10^5$ and $S_{eff} = 10^7$ have been taken where the voltage across the junction V_s has been chosen 0.725 V. The minority carrier density p(x) at the low-high interface ($n^- n^+$) depends upon the effective surface recombination velocity S_{eff}. Hole concentration at the interface increases with decrease of S_{eff}.

3.8 Current voltage characteristics of a Schottky Barrier diode

The model of the present work can be used for obtaining the current as a function of forward bias voltage for three different region of operation namely i) Low-injection, ii) Neglecting recombination within the drift region (Model II) and iii) Considering the recombination (Model I). To generate the plot, following steps have been adopted:

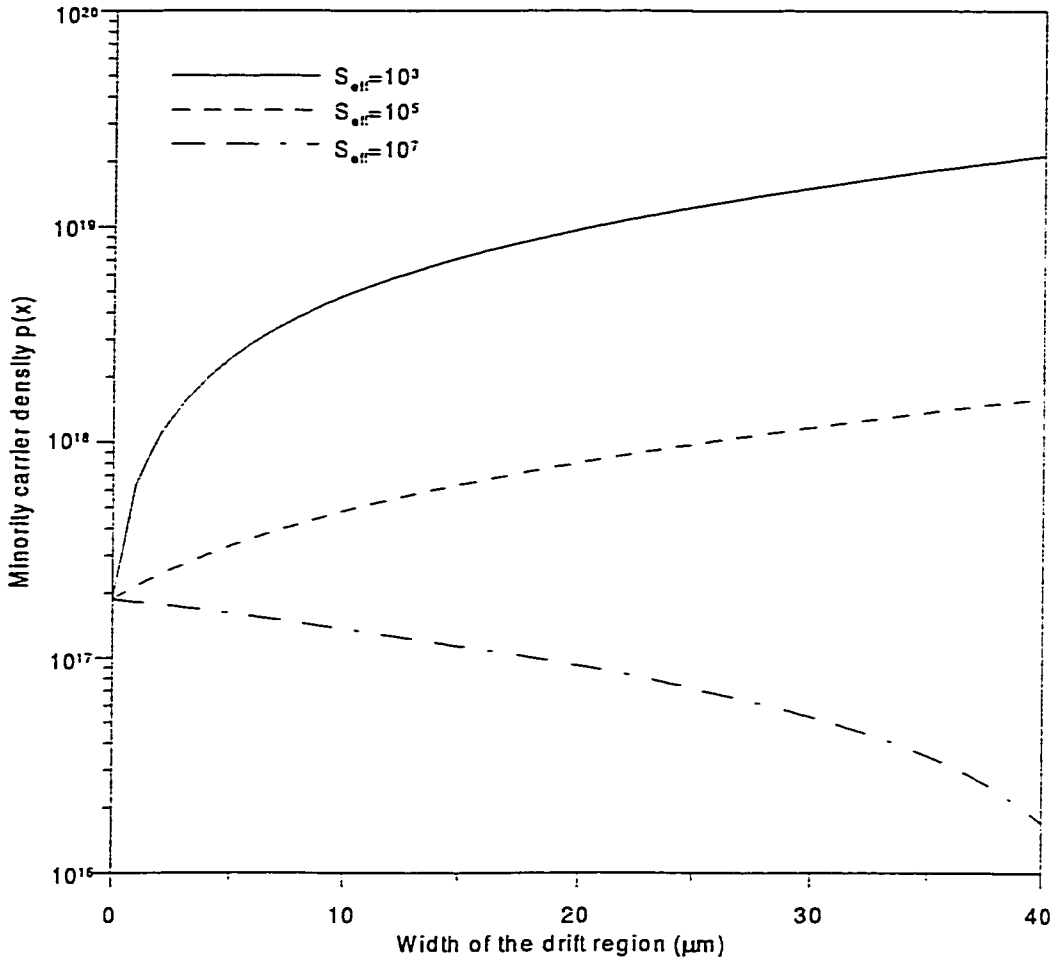

Figure 3.6: Effect of surface recombination velocity on minority carrier concentration.

Step1: A value of the voltage across the junction is chosen.

Step2: The majority carrier current density J_{no} is calculated from equation 3.3 for a given voltage across the junction V_s.

Step3: Hole concentration at x=0, p_o is calculated from equation 3.1 with the computed value of J_{no}.

The region of operation has been decided by comparing the obtained value of p_o with that from equation 2.34 and equation 2.43.

Step4: a. When the condition from equation 2.43 is satisfied then J_{po} is neglected and $J = J_{no}$. Voltage across the drift region V_{inj} is calculated from 2.52. The voltage across the SB diode is obtained from the following equation:

$$V_a = V_s + V_{inj} \tag{3.5}$$

where

$$V_{sub} = J \times R_{sub} \tag{3.6}$$

b. When equation 2.34 is satisfied total current J can be obtained for the case where recombination has been neglected. Hole concentration at the low-high interface $(n^- n^+), p_L$ is obtained from equation 2.41. Here total

current $J = J_{no} + J_{po}$ and total applied voltage is 3.5.

c. If both the conditions are not satisfied, Model I is used for current-voltage characteristics. Hole concentration at x=0, p_o, and majority carrier current density at the same place J_{no} is required for finding minority carrier current at x=0, J_{po}. p_o and J_{no} are obtained from equation 3.1 and 3.3 respectively. The total current J is found from $J = J_{no} + J_{po}$. With known values of p_o and J, V_{inj} is determined from equation 2.30 and equation 2.31 upon satisfying the condition $a^2 < b^2$ or $a^2 > b^2$ respectively.

3.8.1 Low injection

Figure 3.7 shows the current as a function of applied forward voltage V_a. For low injection, current increases with voltage and it is observed that J varies exponentially with forward voltage. At low current density, the effect of voltage drop across the substrate V_{sub} and voltage across the drift region V_{inj} are low in compare with the voltage at the junction V_s. So, in this level of voltage J varies with V_s. J is an exponential function of V_s. As a result, J varies exponentially with V_a. This J-V characteristics for low injection obtained by the proposed model shows the same behaviour obtained in experiments of [6], [5] and [19]. The analytical results obtained by the present model have been compared with experimental data available in the

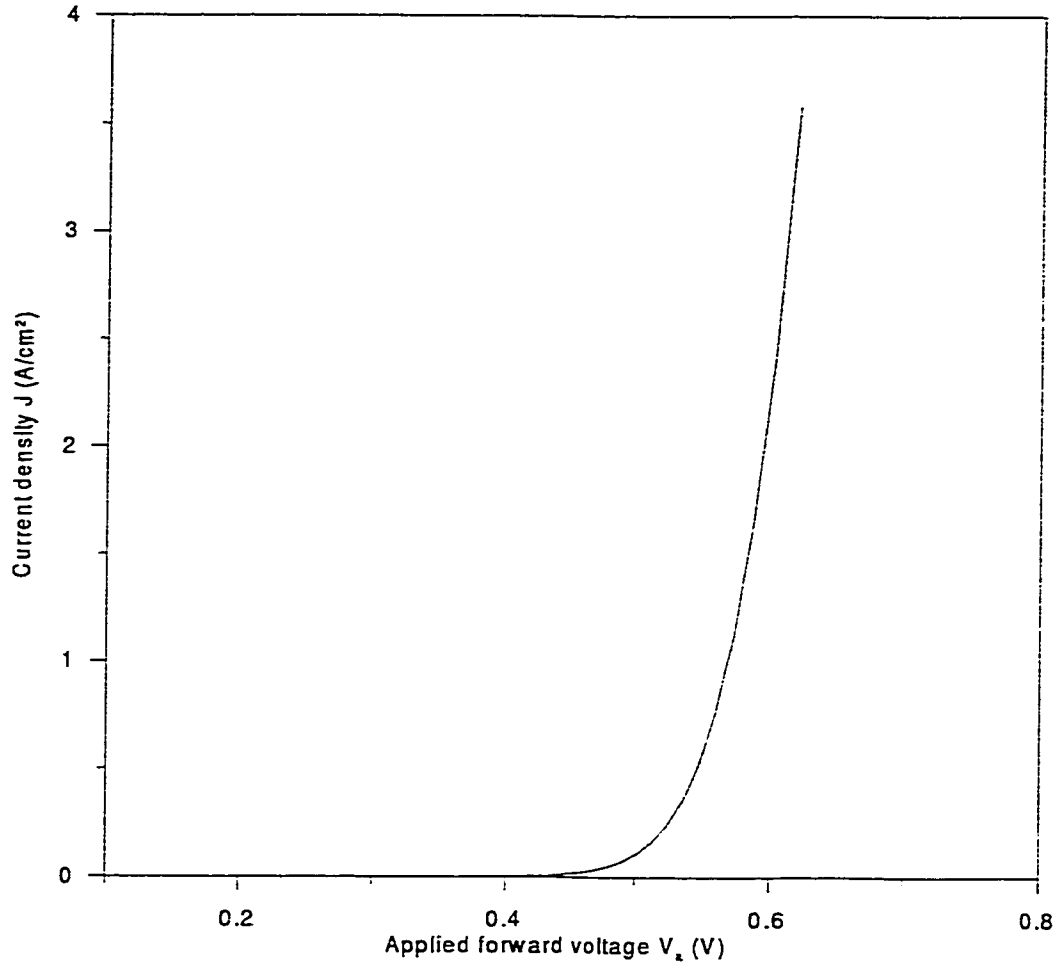

Figure 3.7: J-V Characteristics of an SB diode at low-injection model.

literature of B. Elfsten and P. A. Tove [6]. The J-V characteristics are shown in Figure 3.8. The simulated result are in excellent agreement with experimental data.

3.8.2 Without recombination within the drift region

Current-voltage characteristic neglecting recombination within the drift region is shown in Figure 3.9. The curve shows that the current increases with applied forward voltage V_a and varies exponentially. J_{no} is an exponential function of V_s. At low current densities, V_{inj} and V_{sub} are small compared to V_s and V_a is approximately equal to V_s. But at large current density, V_{inj} and V_{sub} also becomes dominating and V_a cannot be equal to V_s. As a result the current cannot be the exponential function of applied voltage.

3.8.3 With recombination within the drift region

Model I is used to obtain J-V characteristics for the case where recombination within the drift region is not neglected. . Figure 3.10 shows the dependence of J on V_a. At large current density, V_{sub} becomes dominant compared to other two voltages. As a result J-V characteristic follows approximately linear relationship.

3.8.4 Typical SB forward characteristics

In chapter 2 the expressions for p(x), $J_p(x)$ and E(x) are obtained. Using the obtained equations, the current-voltage characteristics of an SB can be studied.

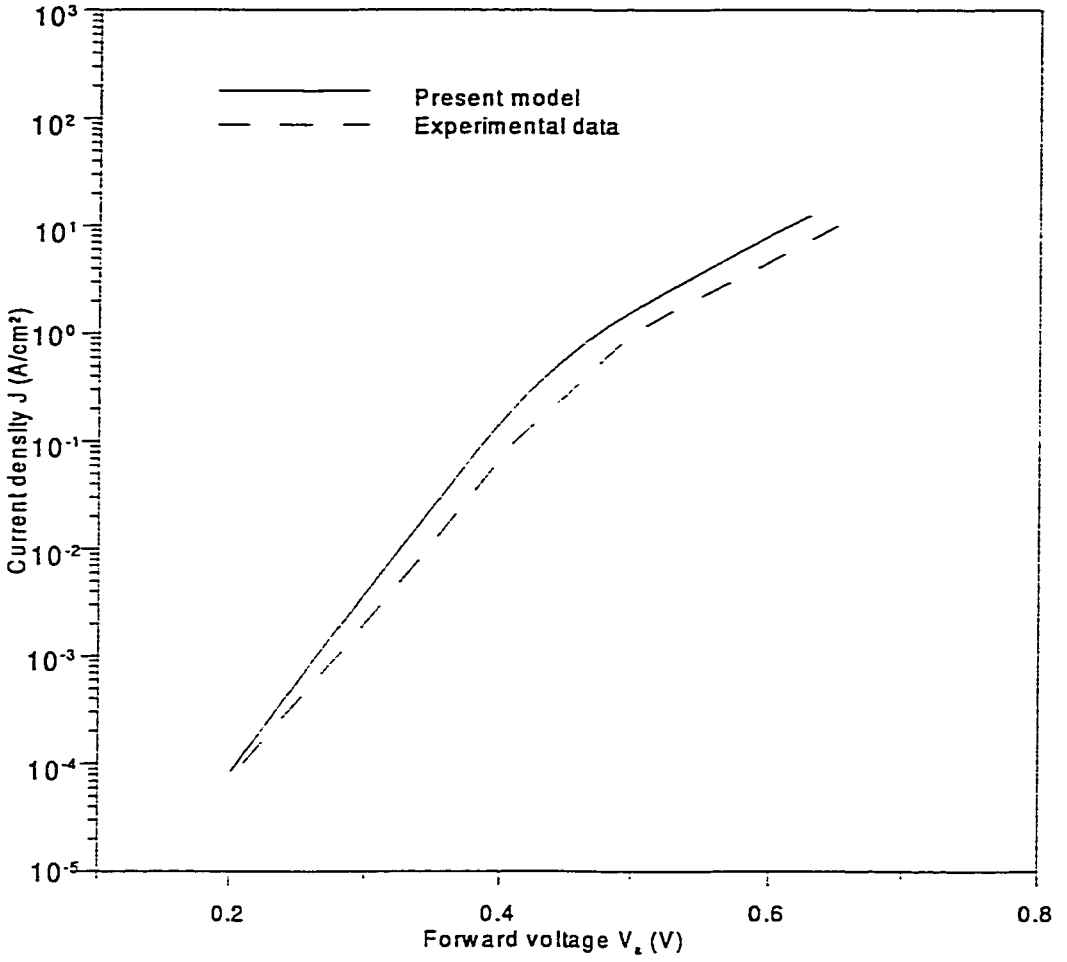

Figure 3.8: Comparison of the J-V characteristic computed from the present model and obtained from measurement reported in [6].

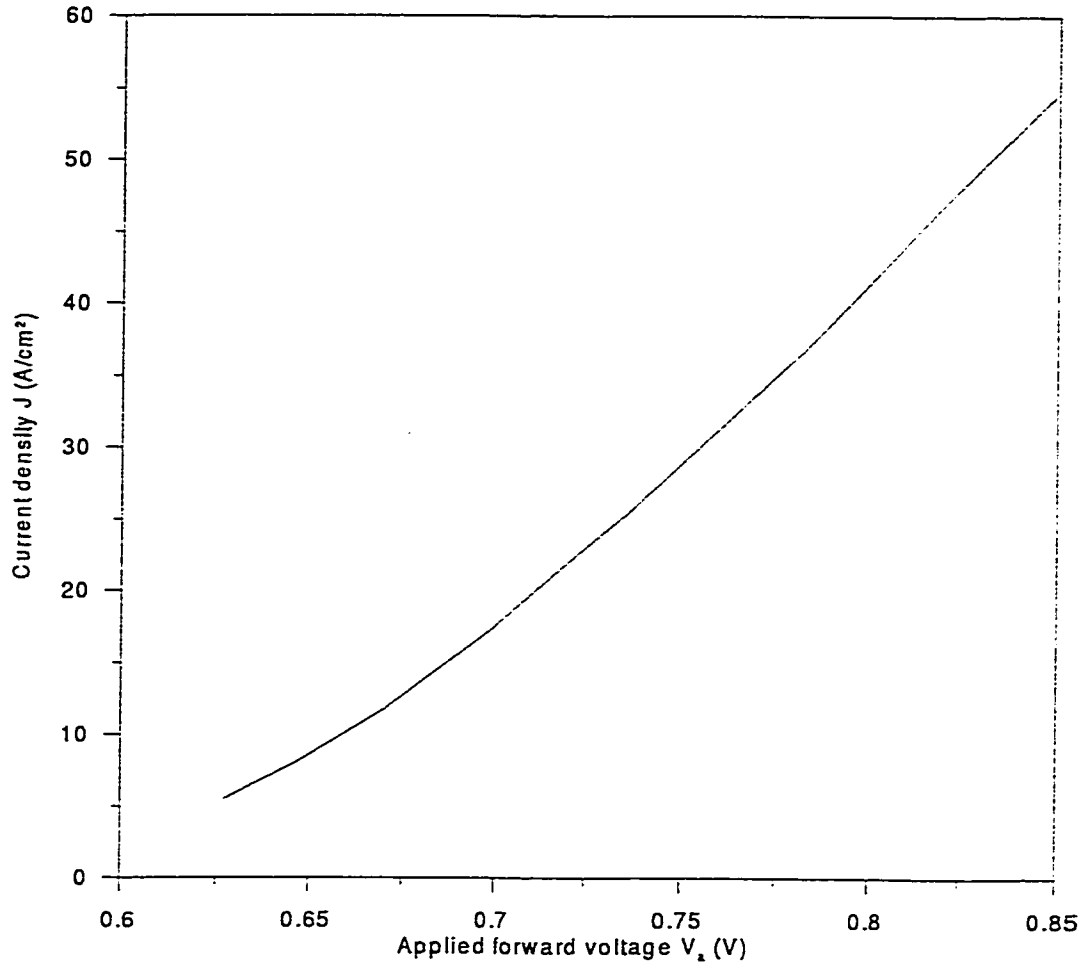

Figure 3.9: J-V Characteristics of an SB diode, neglecting recombination.

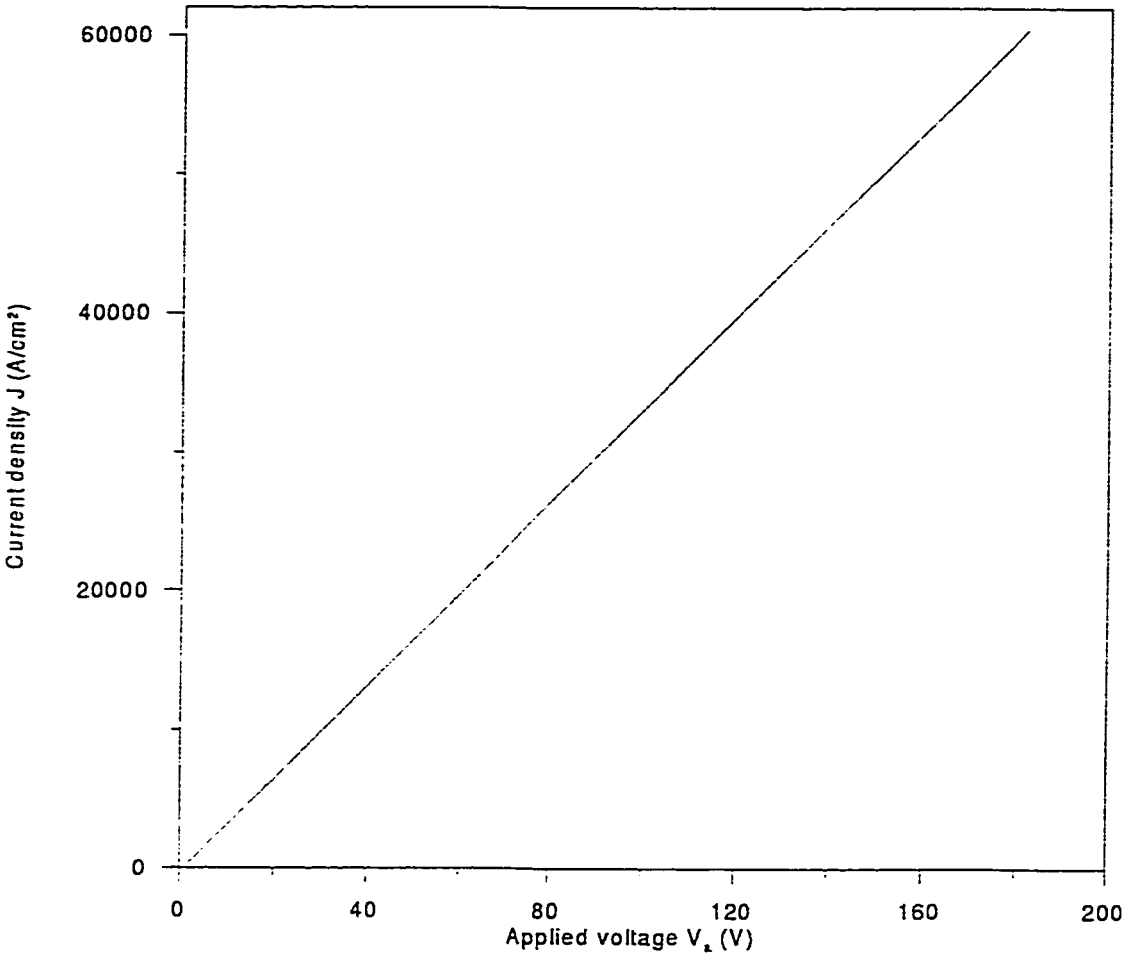

Figure 3.10: J-V Characteristics of an SB diode, considering recombination.

The J-V characteristic has been shown in Figure 3.16 for different width of the drift region. The substrate resistance $R_{sub} = 0.003\Omega - cm^2$ is used. The slope for different levels of injection is different due to following reason:

For low injection, recombination is negligible ,current density is small and J varies exponentially with V_a. At small current density voltage drop across the drift region and ohmic drop at the substrate is too small in comparison with the voltage across the junction. As a result, current becomes exponential function of voltage.

At large current density V_{inj} and V_{sub} becomes significant resulting a slow variation of current density with applied forward voltage (V_a).

Model I and Model II deal with hole recombination current. In Model II, hole recombination current within the drift region is neglected and the hole current due to the recombination at the low-high ($n^- n^+$) interface is considered. Due to this hole current the dependence of total current density J will be different from that for low injection model.

In Model I, the recombination current in the drift region and also recombination at the interface are considered. The model is applicable at large current densities. At large current densities the voltage drop across R_{sub} dominates and is larger than V_s and V_{inj}. This effect flattens the J-V characteristic.

The J-V characteristic obtained by the present model is compared with that without considering minority carrier hole current. With $J_p = 0$, the Schottky Barrier acts as a majority carrier device. It is found that at higher current the model with

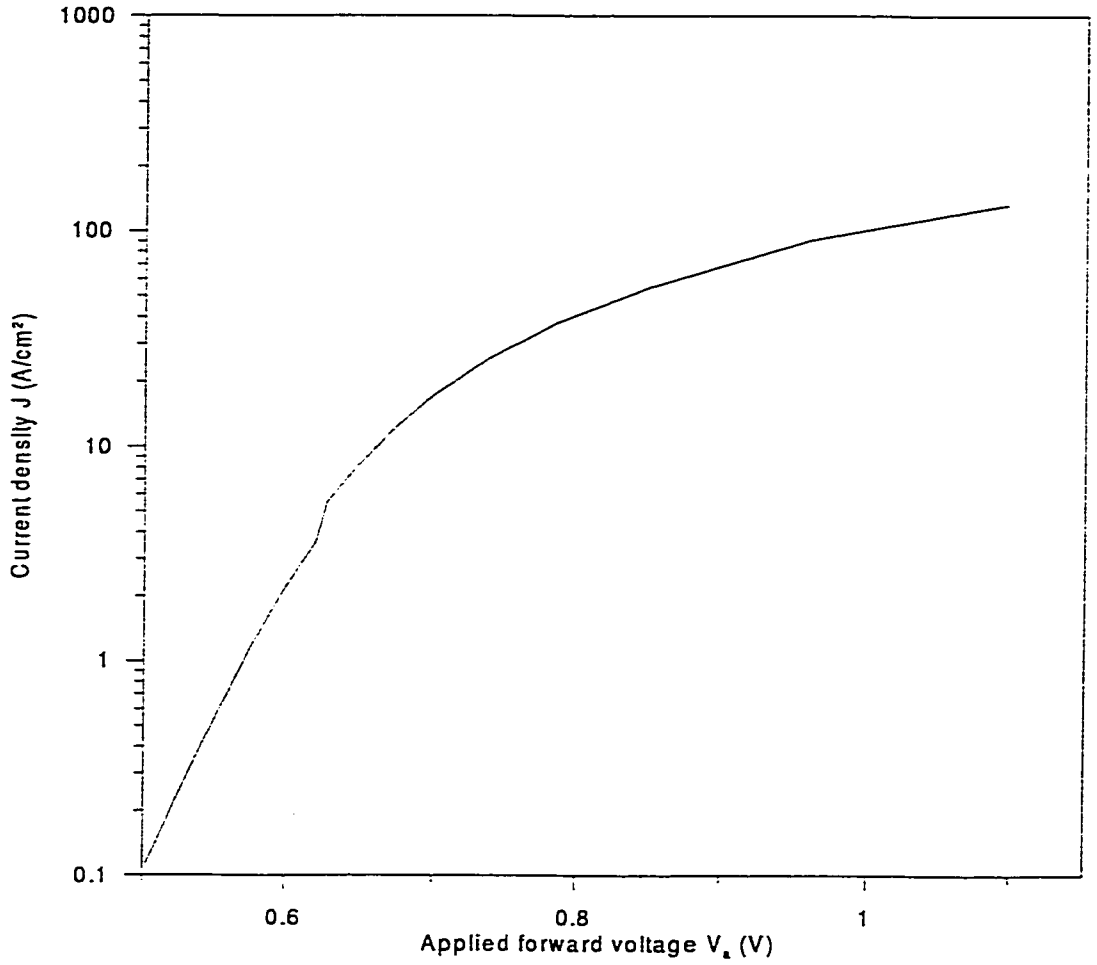

Figure 3.11: J-V Characteristics of an SB diode using the present Model.

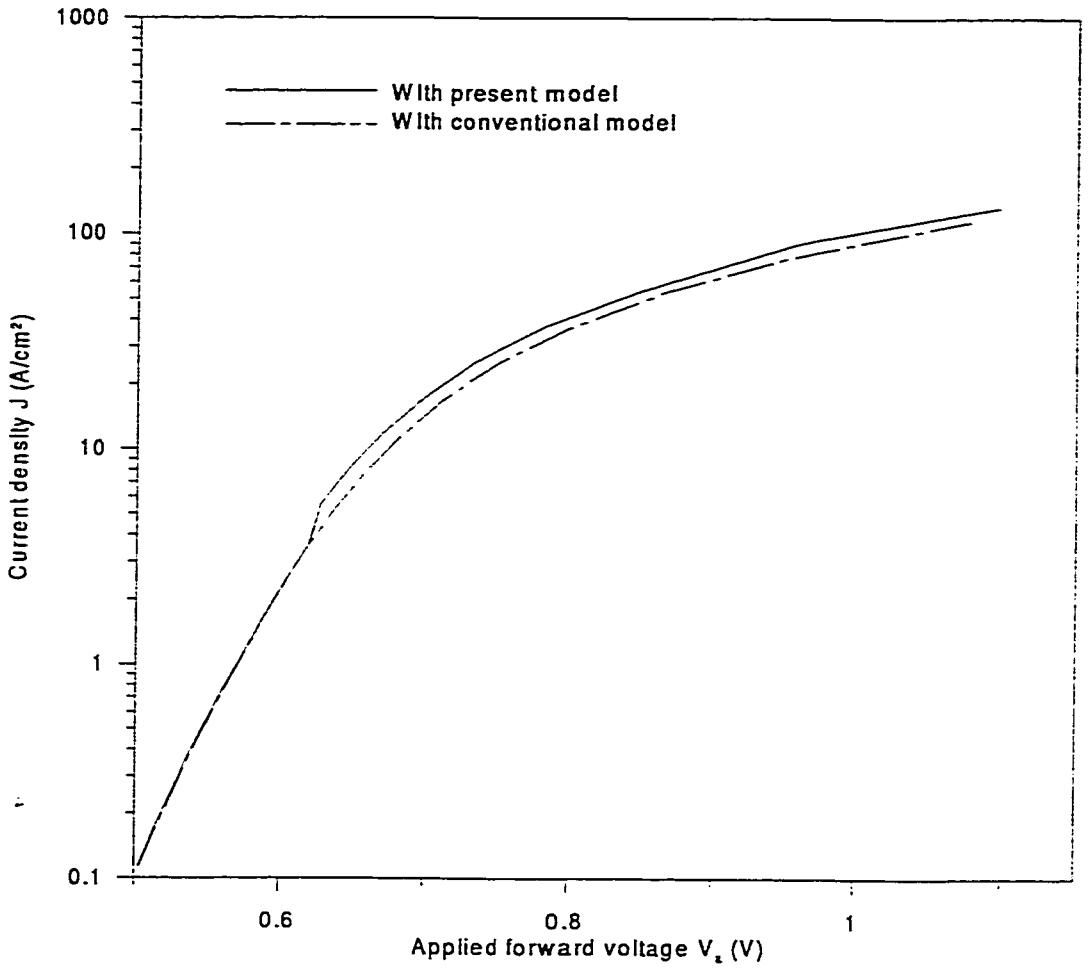

Figure 3.12: Comparison between present and conventional model for a typical J-V characteristic of an SB diode.

recombination differs from the conventional model and is shown in Figure 3.12. The larger the current density the difference in current becomes significant.

The J-V characteristics obtained by experiments [1] and [18] are shown in Figure 3.13. As the device parameters and device makeups are not provided in [1] and [18], the comparison was not possible. However the present model and the experiment shows the similar dependence of J on V_a.

The SB with low barrier height can be considered as a majority carrier device. But an SB with high barrier height, injects minority carriers at low applied voltage. The ratio $\frac{J_{no}}{J_{po}}$ for two different values of barrier height is shown in Figure 3.15. The hole current density becomes significant for an SB with high barrier height.

Figure 3.14 shows J-V characteristic for three different doping densities while Figure 3.16 shows J-V characteristic for three different width of the drift region. The dependence of J on V_a with different doping densities is small. On the other hand the current density J varies with L_d. It is observed that J increases with L_d. For a given V_s, J_{no} is constant but J_{po} depends upon L_d. J_{po} increases with L_d resulting in total increase in the current density J.

Dependence of effective surface recombination velocity S_{eff} on J is also studied in the present work. Figure 3.17 shows that current increases with S_{eff} for a given V_a. For a given N_d and L_d, the recombination at the low-high (n^-n^+) interface increases with S_{eff} and this results in total increase of J.

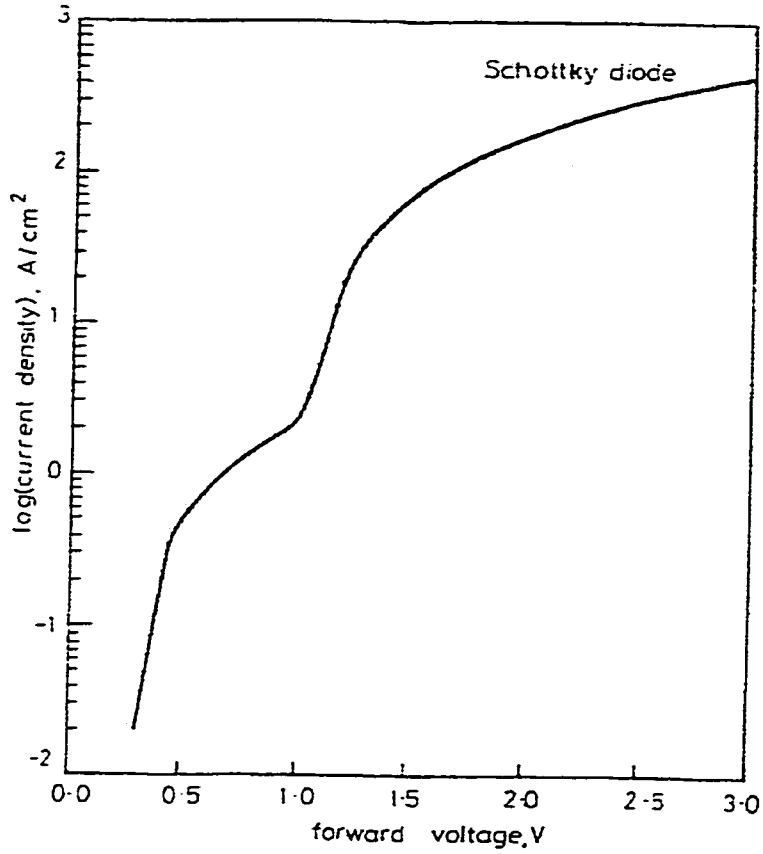

Figure 3.13: A typical J-V characteristic of an SB diode shown in [18].

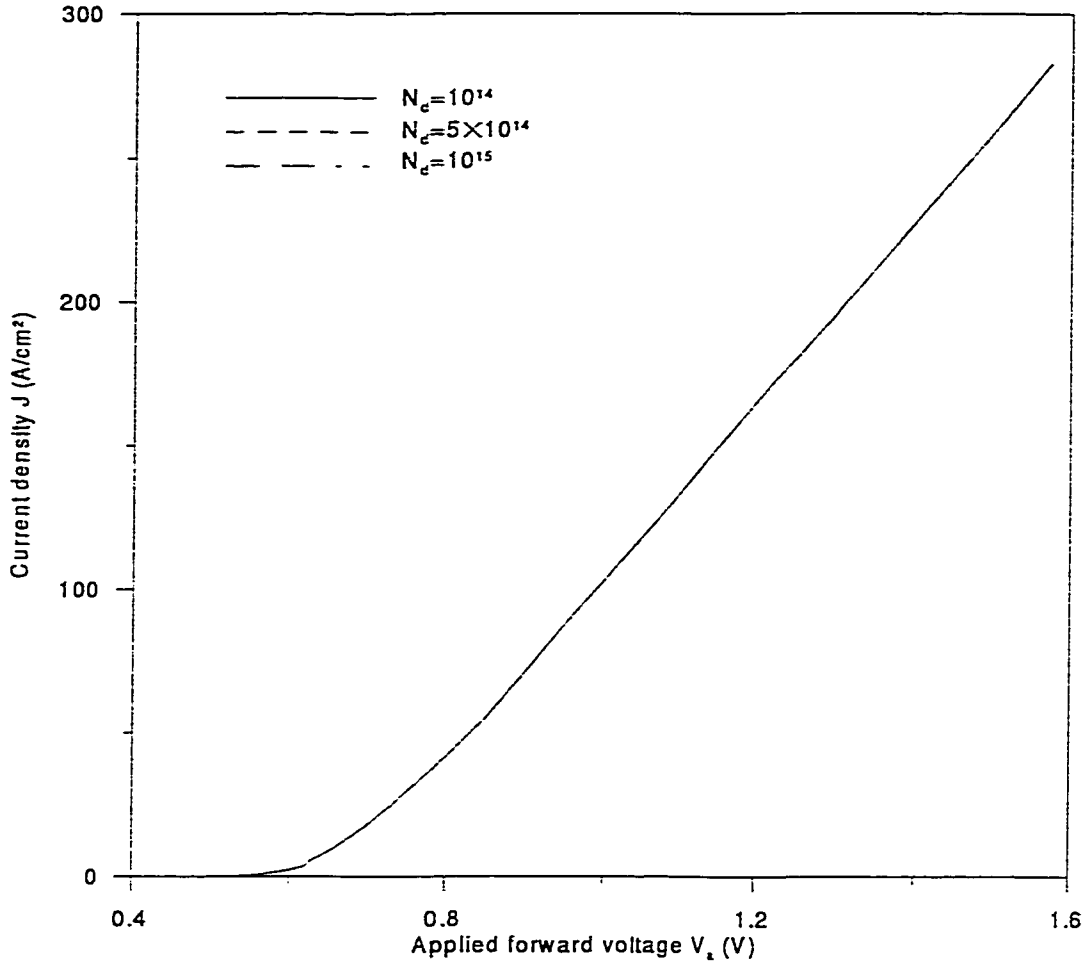

Figure 3.14: J-V characteristic of an SB diode for different doping densities.

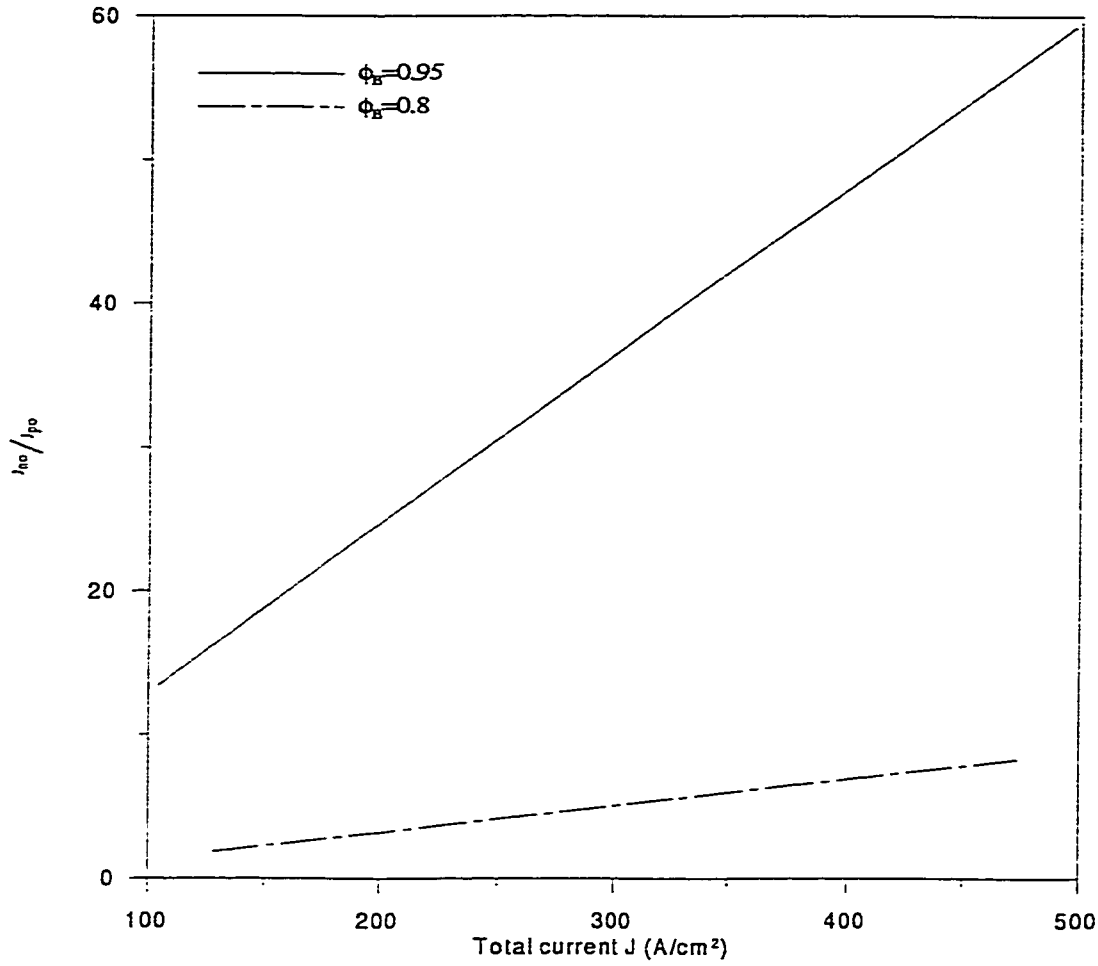

Figure 3.15: Ratio of electron and hole current densities for different barrier height.

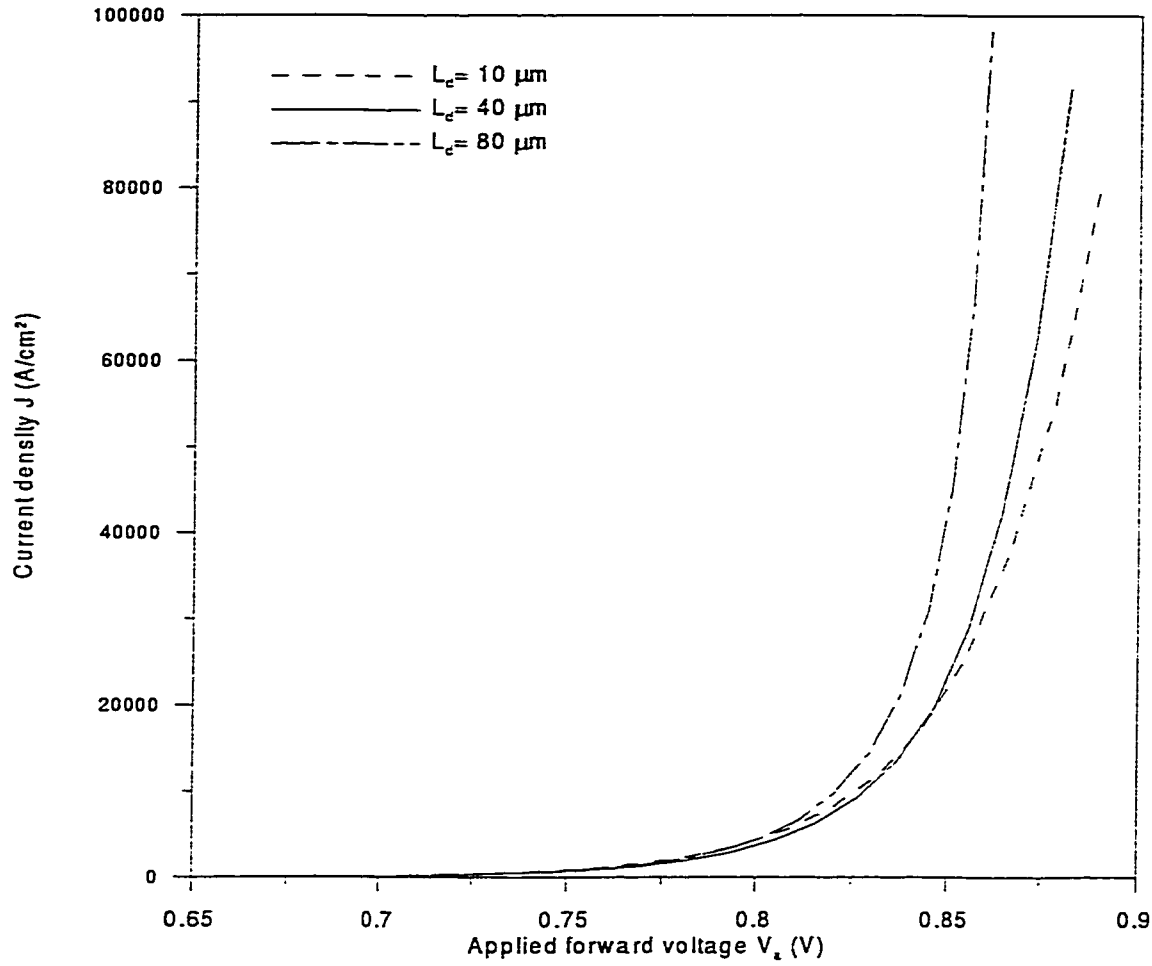

Figure 3.16: J-V characteristic of an SB diode for different lengths of the drift region.

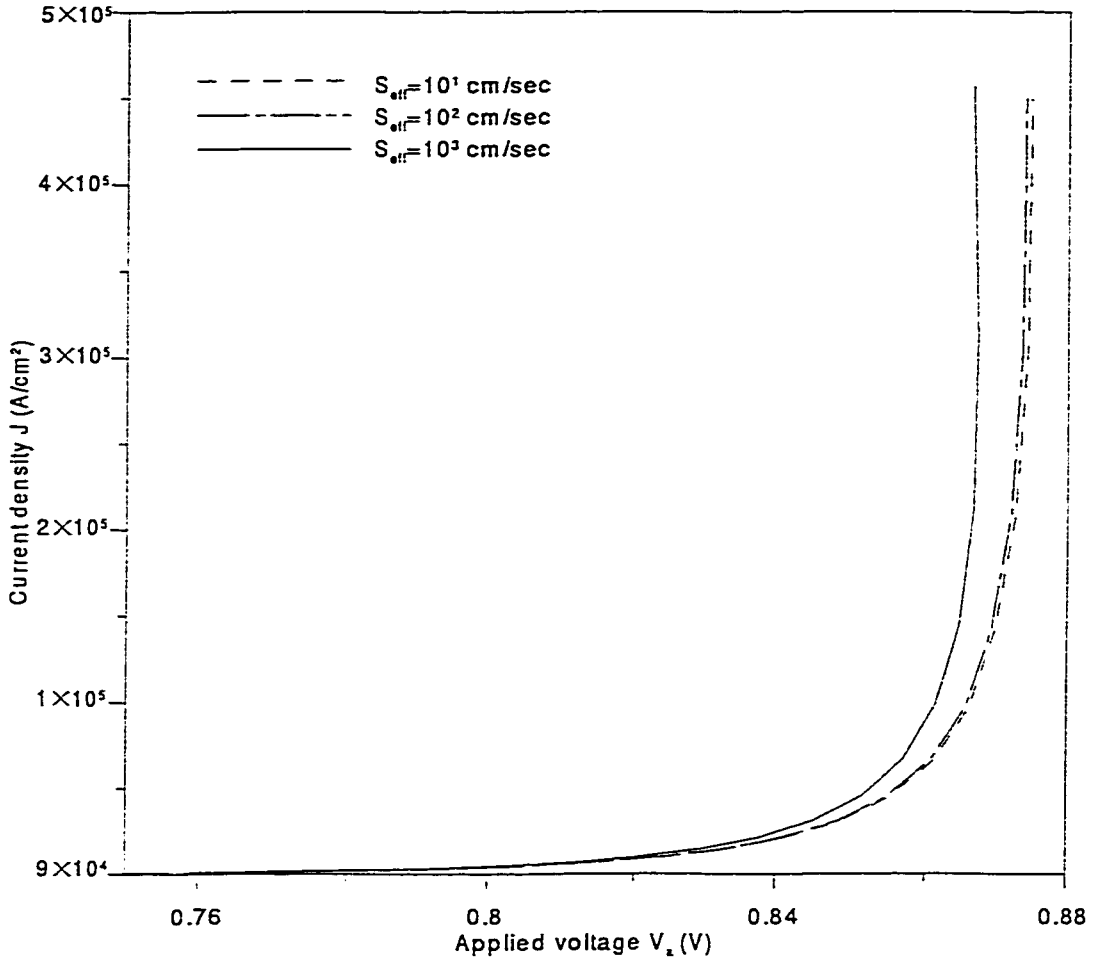

Figure 3.17: J-V characteristic of an SB diode with different effective surface recombination velocities.

3.9 Injection ratio

Injection Ratio γ as a function of forward current density J, for three different width of the drift region L_d is plotted in Figure 3.18 and in Figure 3.19. The electron current density J_{no} depends upon V_s and it is an exponential function of V_s. The hole current density J_{po} also increases with V_s but its dependence on V_s is not exponential. The ratio $\frac{J_{no}}{J_{po}}$ increases and γ decreases with V_a. The behavior is also supported by experiments [[6]; fig.(11)] and [[6]; fig.(12)].

It is also found that γ increases with L_d due to increase in J_{po} shown in Figures 3.18 and 3.19. This increase in J_{po} causes increase in J with L_d.

To study the dependence of γ on S_{eff}, γ vs J for three different values of S_{eff} is plotted in Figures 3.20 and 3.21. For a given S_{eff}, γ decreases with J. Even though, J_{po} increases with J but the ratio $\frac{J_{po}}{J_{no}}$ decreases and as a result γ decreases. With increase of S_{eff}, the current density J_{pL} which results increase in J_{po} and γ also increases.

The dependence of γ on J for three different doping densities is shown in Figures 3.22 and 3.23. At low current densities γ decreases with increase of doping density N_D. For a given V_s, p_o decreases with N_D and the recombination within the drift region decreases. The high injection situation occurs when $p_o \gg N_D$ and the hole current becomes almost independent of N_D at large current density.

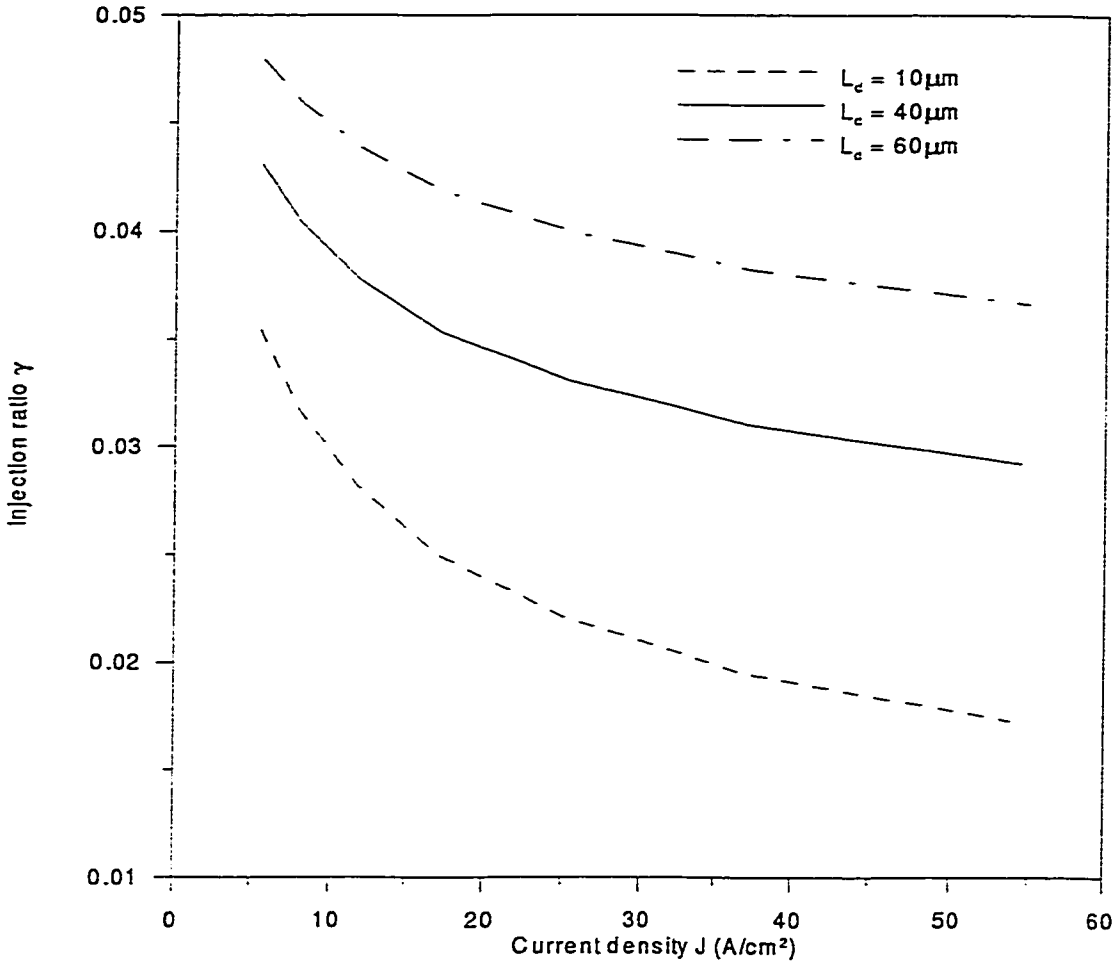

Figure 3.18: Injection ratio as a function of forward current density for Model II with different widths of the drift region.

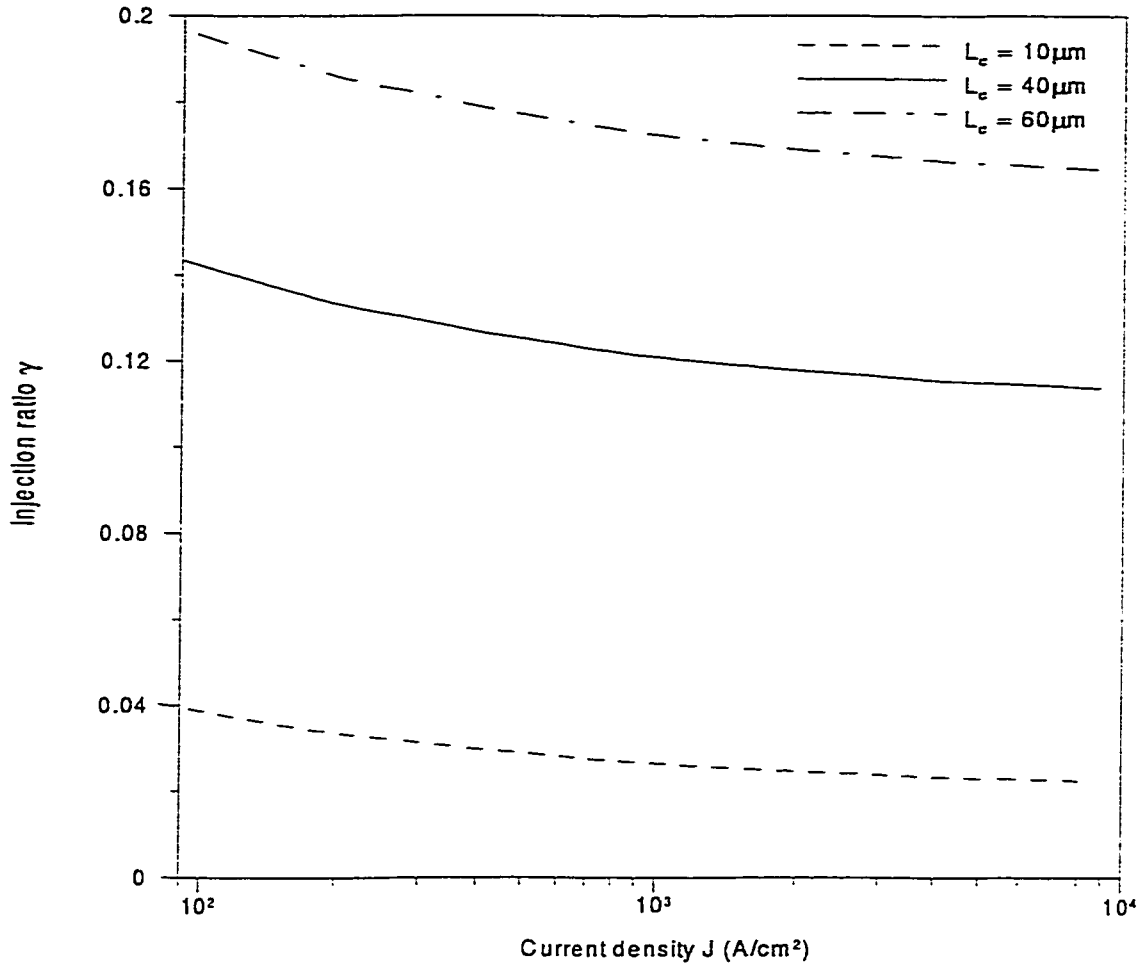

Figure 3.19: Injection ratio as a function of forward current density for Model I with different widths of the drift region.

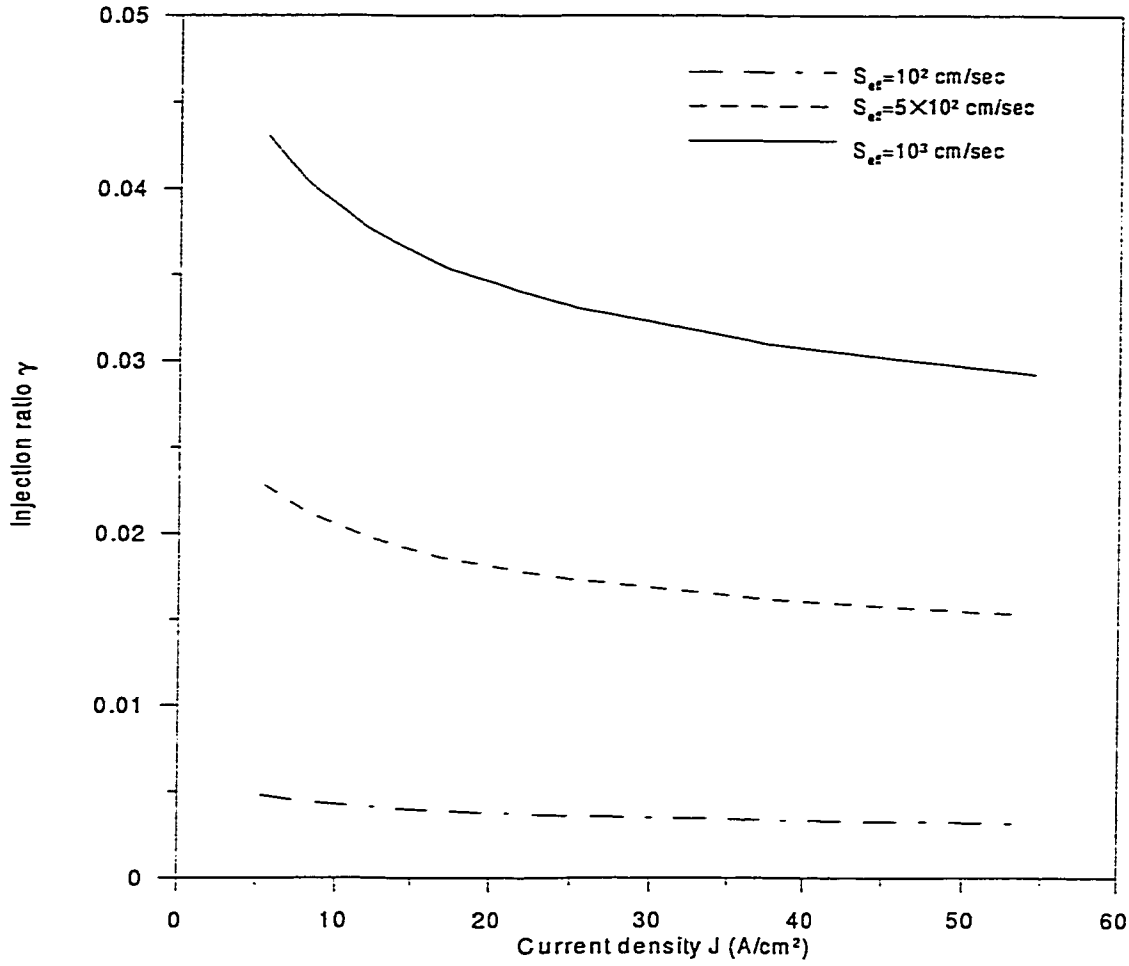

Figure 3.20: Injection ratio as a function of forward current density for Model II for different effective surface recombination velocities.

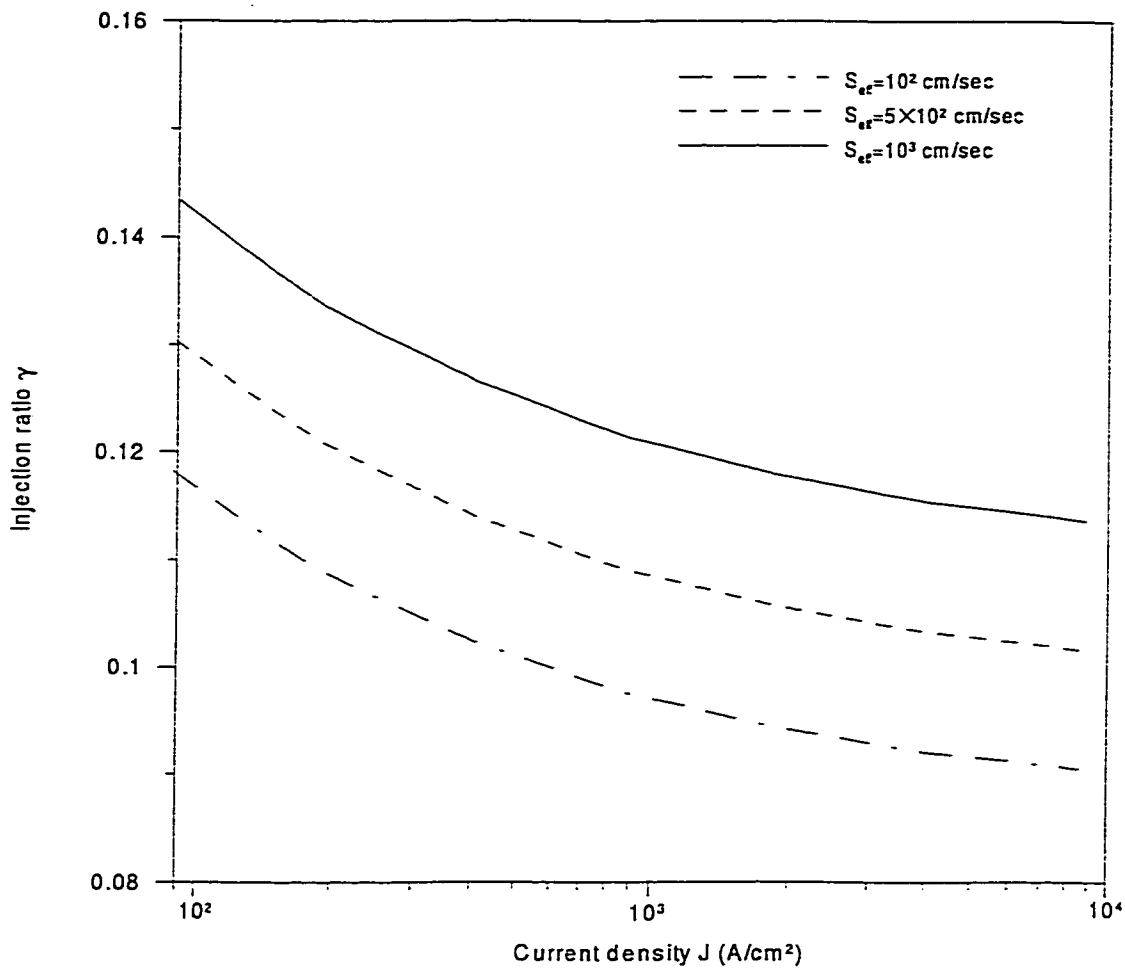

Figure 3.21: Injection ratio as a function of forward current density for Model II for different effective surface recombination velocities.

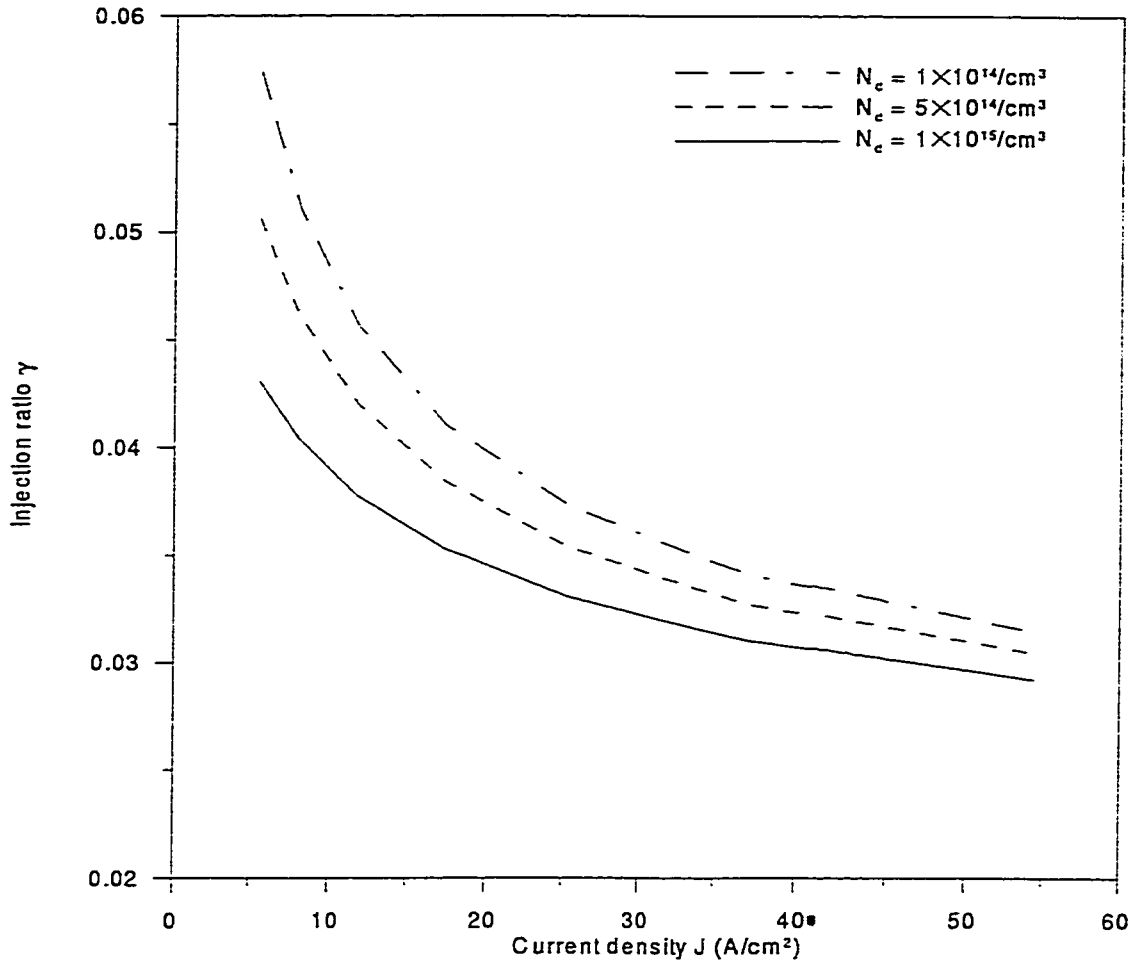

Figure 3.22: Injection ratio as a function of forward current density for Model II with different doping densities.

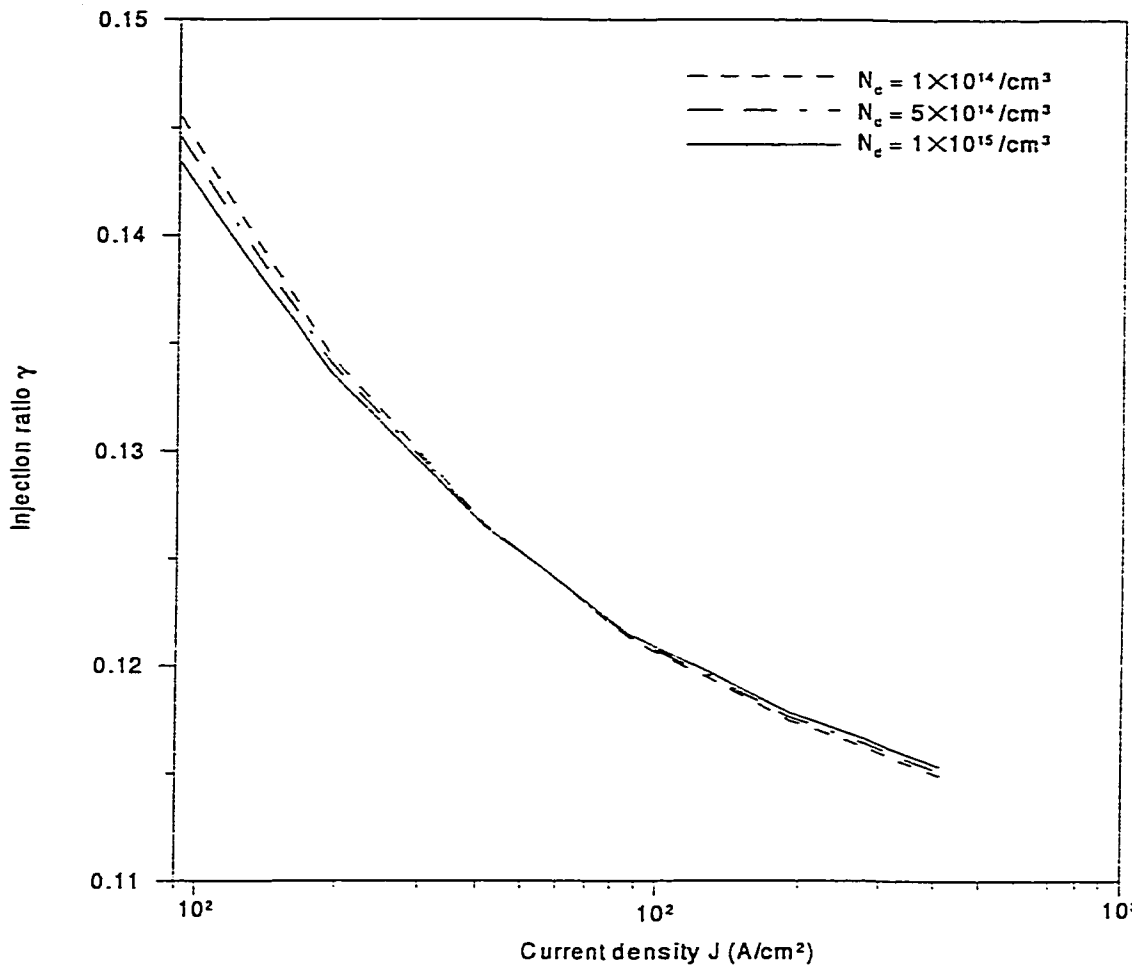

Figure 3.23: Injection ratio as a function of forward current density for Model I with different doping densities.

3.10 Charge storage time

Storage time as a function of J is plotted in Figures 3.24, 3.25 and 3.26. In the computational work τ_s is obtained from the relation,

$$\tau_s = \frac{Q_s}{J_r} \tag{3.7}$$

where J_r is the reverse current density. $J_r = 600A/cm^2$ is used in this work.

Figure 3.24 shows τ_s as a function of J for three different widths of the drift region. τ_s follows a linear relationship with J and this linear behaviour of storage time with J was also observed in experiment [fig. 10; [6]]. τ_s increases with L_d because Q_s increases with L_d.

Figure 3.24 shows the dependence of storage time τ_s on effective surface recombination velocity. At low surface recombination velocity S_{eff}, the stored charge increases significantly due to the blocking properties of the minority carrier of low-high ($n^- n^+$) interface and this increase in stored charge causes a large increase in storage time. For high injection levels, the minority carriers are not supply limited and a larger recombination velocity would help to remove minority carriers and reduce the storage time.

The dependence of storage time on N_D is not significant as is evident from plots shown in Figure 3.26. At large current density Q_s is independent of N_D and as a result τ_s is also independent of N_D.

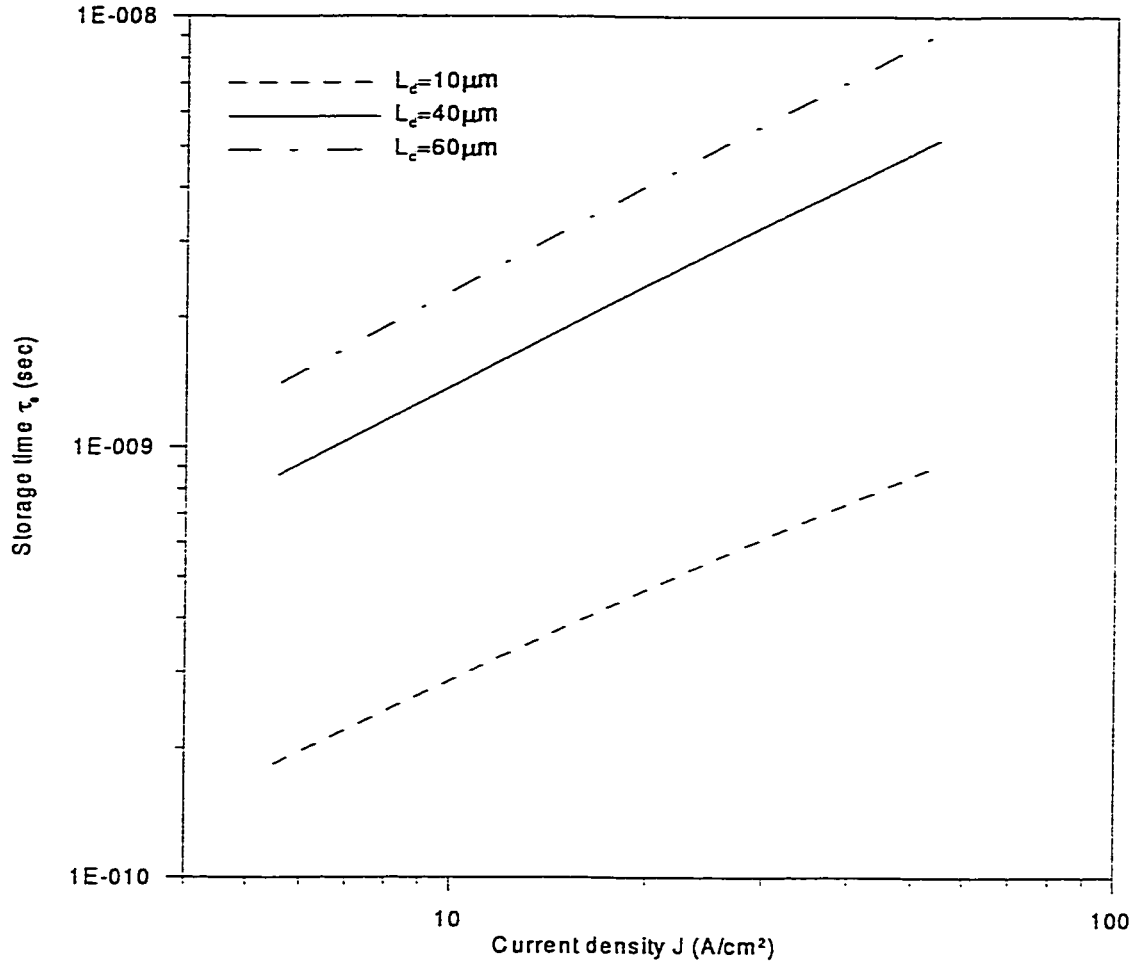

Figure 3.24: Storage time as a function of forward current density for different widths of the drift region.

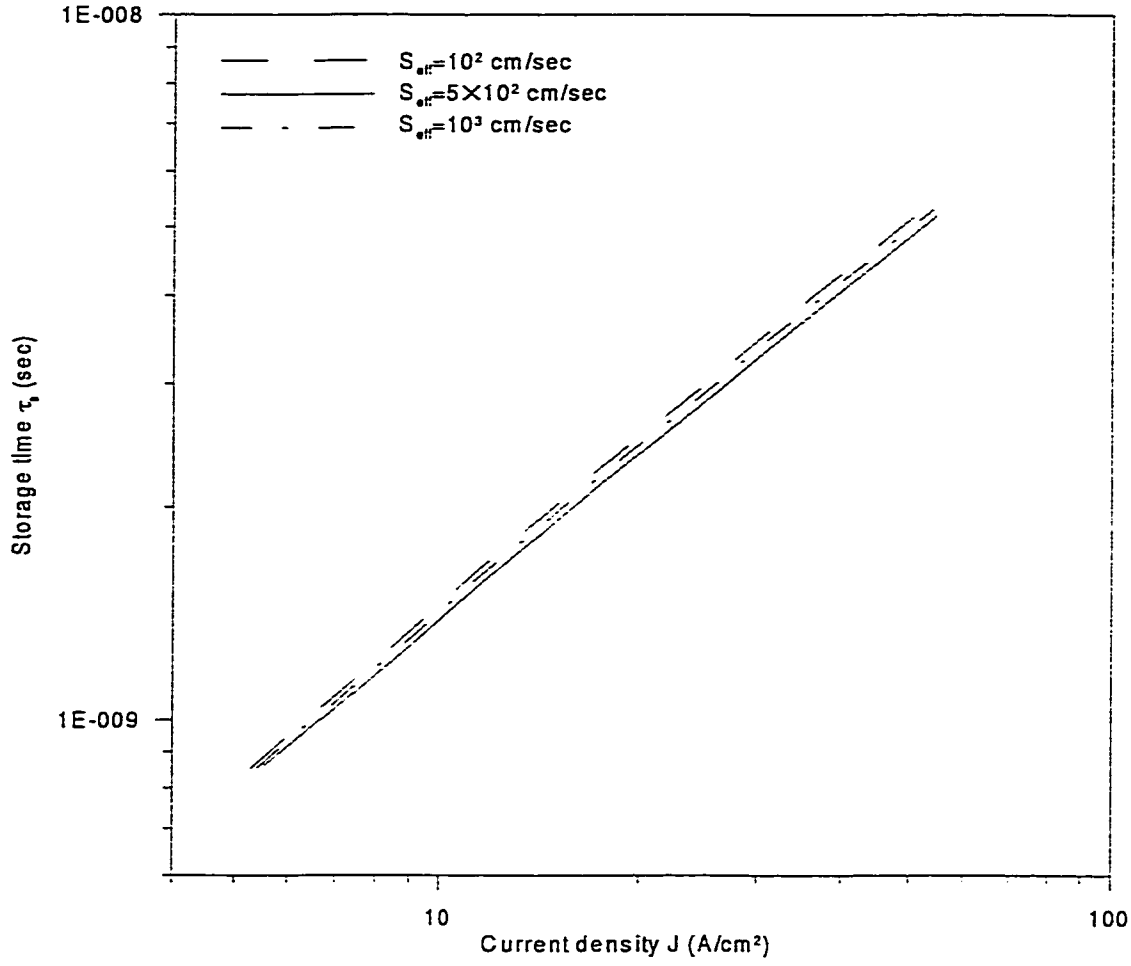

Figure 3.25: Storage time as a function of forward current density for different effective surface recombination velocities.

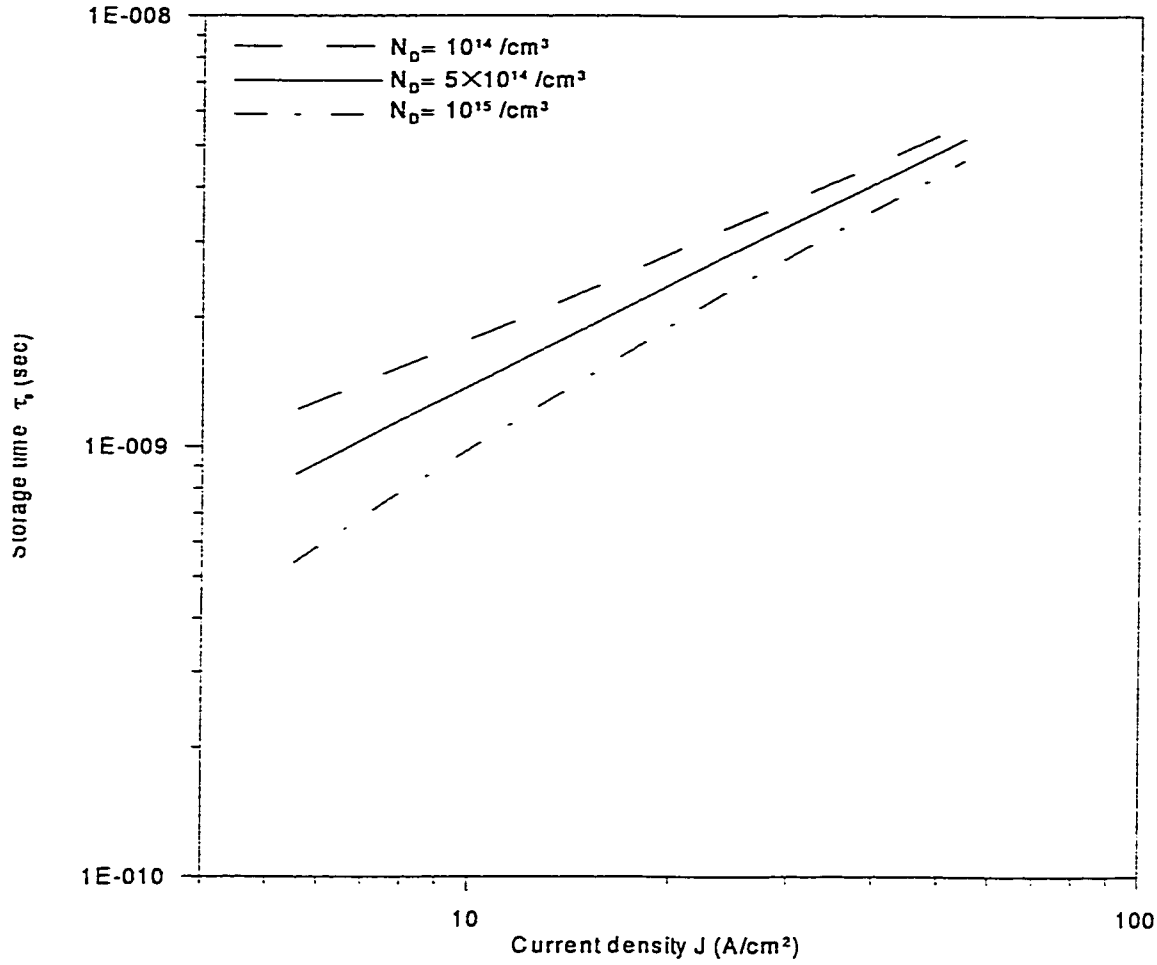

Figure 3.26: Storage time as a function of forward current density for different doping densities.

3.11 Conclusion

The different characteristics of an epitaxial Schottky Barrier diode have been studied by using the model proposed in this thesis. In the model the dependence of the minority carrier lifetime and effective surface recombination on minority carrier concentration have been studied. A boundary condition that determines the operation of the diode in between high and intermediate region and another condition for operation between intermediate and low region are proposed. In high injection recombination within the drift region and minority carrier blocking properties of the low high interface are considered. In intermediate region only the blocking properties of the interface is considered. In low injection minority carrier current is neglected. The results obtained using the present model is compared with the conventional model where minority carrier hole current was not incorporated. And a noticeable deviation has been observed. The experimental results found in literature have shown a point of change over in the J-V characteristic. The present model is able to explain this type of behaviour in J-V characteristic. Where as, the conventional model has failed to predict this important aspect. The present model is valid for all levels of injection of minority carriers.

Chapter 4

CONCLUSION AND SUGGESTION

4.1 Conclusion

In this work a model is developed for studying the characteristic of Schottky Barrier diode with high barrier height for all levels of injection. Boundary conditions are introduced to combine the Model I with Model II and Model II with low level injection. In model II, minority carrier recombination within the drift region is neglected whereas, model I is developed considering recombination within the drift region. This enables to apply the model over a wide range of current density level. The model is able to provide solution for important physical quantities such as electric field, minority carriers, injection ratio and storage time. In developing the

model, drift-diffusion currents, recombination of carriers are considered. Therefore, this model gives the more accurate result and also gives a better physical insight into the device operation.

4.2 Suggestion

The insight gain form this analysis can be adopted to model more complicated device structure that incorporates the SB diode. The model is developed considering recombination within the drift region. The similar situation will occur when transistor drives into quasi-saturation. The equation obtained in this work can be applied to study the behavior of the bipolar transistor in quasi-saturation mode of operation.

Appendix A

Hole concentration profile for high injection with recombination

Equation for hole concentration profile:

$$p(x) = p_o \cosh \frac{x}{L_a} + D \sinh \frac{x}{L_a} \tag{A.1}$$

From equation 2.21 we get:

$$\begin{aligned} \frac{dp}{dx}|_{x=L_d} &= \frac{mJ - (1+m)J_{pL}}{2qD_p} \\ \Rightarrow 2qD_p \frac{dp}{dx}|_{x=L_d} &= mJ - (1+m)J_{pL} \end{aligned} \tag{A.2}$$

Using 2.20, 2.22 and 2.23 the following is obtained from equation A.2:

$$\begin{aligned} \frac{2qD_p}{L_a}\left[p_o \sinh \frac{L_d}{L_a} + D \cosh \frac{L_d}{L_a}\right] &= mJ - (1+m)qS_{eff}\left[p_o \cosh \frac{L_d}{L_a} + D \sinh \frac{L_d}{L_a}\right] \\ \Rightarrow D &= \frac{mJ - (1+m)qS_{eff}p_o \cosh \frac{L_d}{L_a} - \frac{2qD_p}{L_a}p_o \sinh \frac{L_d}{L_a}}{\frac{2qD_p}{L_a}\cosh \frac{L_d}{L_a} + (1+m)qS_{eff} \sinh \frac{L_d}{L_a}} \end{aligned}$$

$$D = \frac{1}{R}\left[\frac{mJL_a}{2qD_p} - \frac{(1+m)L_aqS_{eff}p_o}{2Dp}\cosh\frac{L_d}{L_a} - p_o\sinh\frac{L_d}{L_a}\right] \quad \text{(A.3)}$$

where

$$R = \cosh\frac{L_d}{L_a} + \frac{(1+m)L_aS_{eff}}{2D_p}\sinh\frac{L_d}{L_a} \quad \text{(A.4)}$$

Putting the value of D from A.3 in equation 2.20 the following expression for p(x) is derived:

$$\begin{aligned} p(x) &= p_o\cosh\frac{x}{L_a} + \frac{1}{R}\left[\frac{mJL_a}{2qD_p} - \frac{(1+m)L_aS_{eff}p_o}{2Dp}\cosh\frac{L_d}{L_a} - p_o\sinh\frac{L_d}{L_a}\right]\sinh\frac{x}{L_a} \\ &= \frac{1}{R}\left[p_o\cosh\frac{L_d}{L_a} + \frac{p_oL_aS_{eff}}{2D_p}\sinh\frac{L_d}{L_a}\cosh\frac{x}{L_a} + \frac{mJL_a}{2qD_p}\sinh\frac{x}{L_a}\right] \\ &- \frac{1}{R}\left[\frac{(1+m)L_aS_{eff}p_o}{2D_p}\cosh\frac{L_d}{L_a}\sinh\frac{x}{L_a} - p_o\sinh\frac{L_d}{L_a}\sinh\frac{x}{L_a}\right] \end{aligned} \quad \text{(A.5)}$$

Rearranging equation A.5 the following can be obtained:

$$p(x) = \frac{1}{R}\left[p_o\cosh\frac{L_d-x}{L_a} + \frac{p_oL_a(1+m)S_{eff}}{2D_p}\sinh\frac{L_d-x}{L_a} + \frac{mJL_a}{2qD_p}\sinh\frac{x}{L_a}\right] \quad \text{(A.6)}$$

Appendix B

Voltage across the injection level for high injection with recombination

Equation 2.1 and 2.2 are used to derive the profile for electric field.

$$\begin{aligned} J = J_n + J_p &= q\mu_n nE + qD_n\frac{dn}{dx} + q\mu_p pE - qD_p\frac{dp}{dx} \\ &= q\mu_n pE\left(\frac{\mu_p}{\mu_n}+1\right) qD_n\left(1-\frac{D_p}{D_n}\right)\frac{dp}{dx} \\ &= q\mu_n pE(1+m) + qD_n(1-m)\frac{dp}{dx} \\ \Rightarrow E(x) &= \frac{J}{q\mu_n(1+m)}\frac{1}{p(x)} + V_T\frac{(1-m)}{(1+m)}\frac{1}{p(x)}\frac{dp}{dx} \end{aligned} \tag{B.1}$$

Voltage across the injection region is obtained by integrating the electric field from

equation B.1 in the following way:

$$V_{inj} = -\int_0^{L_d} E(x)dx$$

$$= -\int_0^{L_d} \left[\frac{J}{q\mu_n(1+m)}\frac{1}{p(x)} + V_T\frac{(1-m)}{(1+m)}\frac{1}{p(x)}\right] dp$$

$$V_{inj}(A) = -\frac{J}{q\mu_n(1+m)}\int_0^{L_d}\frac{1}{p(x)}dx \tag{B.2}$$

and

$$V_{inj}(B) = -V_T\frac{(1-m)}{(1+m)}\int_{p_o}^{p_L}\frac{1}{p(x)}dp \tag{B.3}$$

$$V_{inj}(A) = -\frac{J}{q\mu_n(1+m)}\int_0^{L_d}\frac{1}{p(x)}dx$$

$$= -\frac{J}{q\mu_n(1+m)}\int_0^{L_d}\frac{dx}{a\cosh\frac{x}{L_a} + b\sinh\frac{x}{L_a}} \tag{B.4}$$

where

$$\begin{aligned} a &= p_o\cosh\frac{L_d}{L_a} + \frac{p_oL_a(1+m)}{2D_p}S_{eff}\sinh\frac{L_d}{L_a} \\ b &= \frac{mJL_a}{2qD_p} - p_o\sinh\frac{L_d}{L_a} - \frac{p_oL_a(1+m)}{2D_p}S_{eff}\cosh\frac{L_d}{L_a} \end{aligned}$$

This is a standard form of integration which gives the following results:

When $a^2 < b^2$ the integration gives:

$$V_{inj}(A) = -\frac{JR}{q\mu_np(1+m)\sqrt{b^2-a^2}}\ln\frac{\frac{a\tanh\frac{L_d}{2}+b-\sqrt{b^2-a^2}}{a\tanh\frac{L_d}{2}+b+\sqrt{b^2-a^2}}}{\frac{b-\sqrt{b^2-a^2}}{b-\sqrt{b^2+a^2}}} \tag{B.5}$$

and when $a^2 > b^2$ the integration gives:

$$V_{inj}(A) = -\frac{JR}{q\mu_np(1+m)\sqrt{b^2-a^2}}\frac{\arctan\frac{-a\tanh\frac{L_d}{2L_a}+b}{\sqrt{a^2-b^2}}}{\arctan\frac{b}{\sqrt{a^2-b^2}}} \tag{B.6}$$

The later part of the equation B.3 is,

$$V_{inj}(B) = V_T \frac{(1-m)}{(1+m)} \ln \frac{p_o}{p_L} \tag{B.7}$$

Therefore, the total voltage across the injection region is as follows:

$$V_{inj} = -\frac{JR}{q\mu_n p(1+m)\sqrt{b^2-a^2}} \ln \frac{\frac{a \tanh \frac{L_d}{2} + b - \sqrt{b^2-a^2}}{a \tanh \frac{L_d}{2} + b + \sqrt{b^2-a^2}}}{\frac{b-\sqrt{b^2-a^2}}{b-\sqrt{b^2+a^2}}} + V_T \frac{(1-m)}{(1+m)} \ln \frac{p_o}{p_L} \tag{B.8}$$

and,

$$V_{inj} = -\frac{JR}{q\mu_n p(1+m)\sqrt{b^2-a^2}} \frac{\arctan \frac{-a \tanh \frac{L_d}{2L_a} + b}{\sqrt{a^2-b^2}}}{\arctan \frac{b}{\sqrt{a^2-b^2}}} + V_T \frac{(1-m)}{(1+m)} \ln \frac{p_o}{p_L} \tag{B.9}$$

Appendix C

Minority carrier current profile for high injection with recombination

From euqation 2.15 the following expression is obtained:

$$\begin{aligned} \frac{dp}{dx} &= \frac{mJ-(1+m)J_p}{2qD_p} \\ \Rightarrow 2qD_p\frac{dp(x)}{dx} &= mJ-(1+m)J_p(x) \\ \Rightarrow J_p(x) &= \frac{mJ}{(1+m)}-\frac{2qD_p}{(1+m)}\frac{dp(x)}{dx} \end{aligned} \tag{C.1}$$

Now putting the expression of p(x) in C.1 and differentiating it, the following expression for $J_p(x)$ is obtained:

$$\begin{aligned} J_p(x) = &\frac{mJ}{(1+m)}+\frac{2qD_p}{(1+m)RL_a} \\ &\left[p_o\sinh\frac{L_d-x}{L_a}+\frac{p_o(1+m)L_aS_{eff}}{2D_p}\cosh\frac{L_d-x}{L_a}-\frac{JL_a}{2qD_n}\cosh\frac{x}{L_a}\right] \end{aligned} \tag{C.2}$$

Appendix D

Condition for combining Model I and Model II

Recombination current within the drift region has been considered in Model I whereas, this has been neglected in Model II. It is seen that when $J_{pL} \gg J_{pR}$ occurs in Model I, Model II is reached. Therefore,

$$\begin{aligned} J_{pL} &\gg J_{pR} \\ \Longrightarrow J_{pL} &\gg J_{po} - J_{pL} \\ \Longrightarrow J_{pL} &\gg \frac{J_{po}}{2} \end{aligned} \tag{D.1}$$

Substituting the expression for J_{pL} and J_{po} From equations 2.32 and 2.33 in

D.1the following expression is obtained:

$$\frac{2qS_{eff}}{R}\left[p_o+\frac{mJL_a}{2qD_p}\sinh\frac{L_d}{L_a}\right]\gg\frac{m(R-1)}{m+R)}J_{no}+\frac{2qD_p}{(m+R)L_a}\left[1+\frac{(1+m)L_aS_{eff}}{2D_p}\right]p_o\sinh\frac{L_d}{L_a} \tag{D.2}$$

From equation D.2 the following condition is derived:

$$p_o\gg\frac{\frac{m(R-1)}{m+R)}J_{no}-\frac{mJL_aS_{eff}}{RD_p}\sinh\frac{L_d}{L_a}}{\frac{2qS_{eff}}{R}-\frac{2qD_p}{(m+R)L_a}\left[1+\frac{(1+m)L_aS_{eff}}{2D_p}\right]\sinh\frac{L_d}{L_a}} \tag{D.3}$$

Appendix E

Condition for combining Model II and Low-injection

From equation 2.1 and 2.2 the following expression is found:

$$\left(\frac{J_n}{q\mu_n n} - \frac{J_p}{q\mu_p p}\right) = V_T \left(\frac{1}{n} + \frac{1}{p}\right) \frac{dp}{dx} \tag{E.1}$$

Here the condition is achieved if,

$$\left(\frac{J_n}{q\mu_n n} - \frac{J_p}{q\mu_p p}\right) \gg 0 \tag{E.2}$$

At x=0, $J_n = J_{no}$ and $J_p = J_{po} = J_{pL} = qS_{eff}p_L$. Applying the above condition, E.2 can be written as:

$$mJ_{no} > qS_{eff}\left(\frac{N_D}{p_o} + 1\right) p_L \tag{E.3}$$

Appendix F

Voltage across the injection region for without recombination case

Putting the value of E(x) from equation 2.37 in equation 2.2 the following expression is obtained:

$$J_p = \frac{(J_p + mJ_n)p(x)}{(2p(x) + N_D)} - qD_p\frac{dp}{dx}$$
$$\Rightarrow \frac{dp}{dx} = \frac{(mJ_n - J_p)p(x) - J_pN_D}{qD_p(2p(x) + N_D)} \tag{F.1}$$

Again,

$$V_{inj} = -\int_0^{L_d} E(x)dx$$
$$= -\frac{J_{pL} + mJ_{no}}{q\mu_p}\int_0^{L_d}\frac{1}{2p(x) + N_D}dx$$
$$= -\frac{J_{pL} + mJ_{no}}{q\mu_p}\int_{p_o}^{p_L}\frac{1}{(2p(x) + N_D)}\frac{qD_p(2p(x) + N_D)}{(mJ_{no} - J_{pL})p(x) - JpN_D}dp$$

$$\Rightarrow V_{inj} = \frac{J_{pL} + mJ_{no}}{J_{pL} - mJ_{no}} V_T \ln \frac{p_L - \frac{J_{pL} N_D}{mJ_{no} - J_{pL}}}{p_o - \frac{J_{pL} N_D}{mJ_{no} - J_{pL}}} \qquad \text{(F.2)}$$

Appendix G

Voltage across the injection region for low injection case

This is shown earlier that,

$$V_{inj} = -\int_0^{L_d} E(x)dx \tag{G.1}$$

From equation 2.49 the following expression is obtained:

$$\begin{aligned} \frac{J}{qD_n} &= 2\frac{dp(x)}{dx} + \frac{N_D}{V_T}E(x) \\ \Longrightarrow 2\frac{dp}{dx} &= \frac{J}{qD_n} - \frac{N_D}{V_T}E(x) \end{aligned} \tag{G.2}$$

Equation G.2 can be then expressed as:

$$2\int_{p_o}^{p_L} dp(x) = \frac{J}{qD_n}\int_0^{L_d} dx - \frac{N_D}{V_T}\int_0^{L_d} E(x)dx \tag{G.3}$$

From equation G.3 the following expression is found:

$$2\int_{p_o}^{p_L} dp(x) = \frac{J}{qD_n}\int_0^{L_d} dx - \frac{N_D}{V_T}V_{inj} \tag{G.4}$$

Therefore the final expression of V_{inj} is found as follows:

$$V_{inj} = \frac{V_T}{N_D}\left[2(p_L - p_o) - \frac{JL_d}{qD_n}\right] \tag{G.5}$$

Appendix H

Injection ratio

From equation 2.33 the following expression is found:

$$\begin{aligned}
J_{po} &= \frac{mJ}{(1+m)} + \frac{2qD_p}{(1+m)RL_a}\left[p_o \sinh\frac{L_d}{L_a} + \frac{p_o(1+m)L_aS_{eff}}{2D_p}\cosh\frac{L_d}{L_a} - \frac{JL_a}{2qD_n}\right] \\
&= \frac{mJ}{(1+m)} - \frac{mJ}{(1+m)R} + \frac{2qD_p}{(1+m)RL_a}\left[p_o \sinh\frac{L_d}{L_a} + \frac{p_o(1+m)L_aS_{eff}}{2D_p}\cosh\frac{L_d}{L_a}\right] \\
\Longrightarrow \frac{J_{po}}{J} &= \frac{mJ(R-1)}{(1+m)R} + \frac{2qD_p}{(1+m)RL_a}\left[p_o \sinh\frac{L_d}{L_a} + \frac{p_o(1+m)L_aS_{eff}}{2D_p}\cosh\frac{L_d}{L_a}\right] \\
\Longrightarrow \gamma &= \frac{mJ(R-1)}{(1+m)R} + \frac{2qD_p}{(1+m)RL_a}\left[p_o \sinh\frac{L_d}{L_a} + \frac{p_o(1+m)L_aS_{eff}}{2D_p}\cosh\frac{L_d}{L_a}\right] \qquad \text{(H.1)}
\end{aligned}$$

Bibliography

[1] Yoshihito Amemiya and Yoshihiko Mizushima. Bipolar-mode schottky contact and applications to high-speed diodes. *IEEE Transaction on Electron Devices*, ED-31(1):35–41, 1984.

[2] C. Barret and P. Muret. Relation between current-voltage characteristics and interface states at metal-semiconductor interfaces. *Applied Physics Letter*, 42:890–892, 1983.

[3] H. A. Bethe. Theory of the boundary layer of crystal rectifiers. *MIT Radiation Laboratory Report*, 43:12, 1942.

[4] C. T. Chuang. On the minority charge storage for an epitaxial schottky-barrier diode. *IEEE Transaction on Electron Devices*, ED-30(6):700–705, 1983.

[5] Daniel Donoval. Vladimir Drobny and Marek Luza. A contribution to the analysis of the i-v characteristics of schottky structures. *Solid-State Electronics*, 42(2):235–241, 1998.

[6] B. Elfsten and P. A. Tove. Calculation of charge distributions and minotiry carrier injection ratio for high barrier schottky diodes. *Solid-State Electronics*, 28(7):721–727, 1985.

[7] M. P. Godlewski and C. R. Baraona. H. W. Brandliorst. Low-high injection theory applied to solar cells. *Solar Cells*, 29:134–150, 1990.

[8] M. M. Shahidul Hassan. Modelling of lightly doped collector of a bipolar transistor operating in quasi-saturation region. *International Journal for Electronics*, 86(1):1–14, 1999.

[9] Narain D. Arora. John R. Hauser. and David J. Roulston. *IEEE Transaction on Electron Devices*, 41:484, September 1994.

[10] Mike Los Kocsis. *High-Speed Silicon Planar-Epitaxial Switching Diodes.* John Wiley and Sons, 1976.

[11] M. Jagadesh Kumar and K. N. Bhat. Collector recombination lifetime from the quasi-saturation analysis of high-voltage bipolar transistor. *IEEE Transaction on Electron Devices*, 37:2395–2397, 1990.

[12] E. Langer and S. Selberherr. A numerical analysis of bulk-barrier diodes. *Solid-State Electronics*, 25(4):317–324, 1982.

[13] Richard S. Muller and Theodore I. Kamins. *Device Electronics for Integrated Circuits.* John Wiley and Sons, 2nd edition, 1986.

[14] Spirito P. and Cocorullo G. A measurement technique to obtain the recombination lifetime profile in epi layers at any injection level. *IEEE Transaction on Electron Devices*, ED-35:2546–2554, 1987.

[15] Y. P. Pai and H. C. Lin. Current transport in an ion-implantd diode. *Solid-State Electronics*, 24(10):929–934, 1981.

[16] D. L. Scharfetter. Minority carrier injection and charge storage in epitaxial schottky-barrier diodes. *Solid-State Electronics*, 8:299–311, 1965.

[17] B. L. Sharma. *Metal-semiconductor Schottky Barrier Junctions and Their Applications*. Plenum Press, 1st edition, 1984.

[18] J. K. O. Sin and C. A. T. Salama. The sinfet: A new high conductance, high switching speed mos-gated transistor. *Electronics Letters*, 21(24):1134–1136, 1985.

[19] L. Stolt and P A Tove. K. Bohin. Schottky rectifiers on silicon using high barriers. *IEEE Transaction on Electron Devices*, 26(4):295–297, 1983.

[20] Beng G. Streetman. *Solid State Electronic Devices*. Prentice Hall Inc., 2nd edition, 1980.

[21] S. M. Sze. *Physics of Semiconductor Devices*. Wiley Eastern Limited, 2nd edition, May 1993.

[22] A. H. Wilson. The theory of electronic semiconductors. *Proc. R. Soc. Lond. Ser. A*, pages 133–458, 1931.

VITA

- Shaikh Hasibul Majid.
- S/O Arch. Shaikh Abdul Mazid
- Born in Dhaka, Bangladesh on the 21st of March, 1973.
- Received Bachelor's Degree in Electrical & Electronic Engineering from Bangladesh University of Engineering & Technology (BUET), Dhaka in July 1997.
- Completed Master's Degree in Electrical Engineering from King Fahd University of Petroleum & Minerals, Dhahran, Saudi Arabia in May, 2000.